B3: Quantum Atomic and Molecular Physics

Toby Adkins

June 19, 2017

Contents

1. *Introduction*

We shall introduce the basic framework involved in treating multiple-electron atoms, extending the material of the A3: Quantum Mechanics course last year. In particular, we shall cover:

- A recap of hydrogenic atoms
- An upgraded Hamiltonian

At this stage, it might be worth clarifying some of the notational conventions that are going to be used in this text, as they often differ from those used in more standard textbooks. In most textbooks, quantum mechanical operators are referred to using a vector capital, with their single particle eigenvalues being denoted by the corresponding lower case letter, and any composite eigenvalues (such as the sum of angular momenta) being denoted by a non-vector capital. For the total angular momentum, one would typically see

$$\begin{aligned}&\mathbf{J} - \text{operator}\\&j - \text{single particle eigenvalue}\\&J - \text{composite eigenvalue}\end{aligned}$$

This is the notation that we shall adopt in this text, to be consistent with the notation used almost everywhere else.

1.1 A recap of hydrogenic atoms

Before launching into the new material, we shall recap on some of the important results and derivations associated with the quantum mechanical treatment of hydrogenic atoms, in order to familiarise the reader again with the subject, as well as put all of the useful results worth remembering in one place. If the reader already feels comfortable with this material, they can skip straight to section 1.2.

1.1.1 The Hamiltonian and simplifications

Let M and P be the mass and momenta of the centre of mass of the system respectively, and $\mathbf{r} = \mathbf{r}_e - \mathbf{r}_n$, where the subscripts e and n denote the electron and the nucleus respectively. Then, we can write the Hamiltonian of the system as

$$H = \frac{p_e^2}{2m_e} + \frac{p_n^2}{2m_n} + V(r_e - r_n) = \underbrace{\frac{P^2}{2M}}_{\text{centre of mass motion}} + \underbrace{\frac{p^2}{2\mu} + V(\mathbf{r})}_{\text{relative mass motion}} \tag{1.1}$$

where μ is the *reduced mass* of the system. We can arbitrarily choose to move to a coordinate system in which there is no motion of the centre of mass, such that $P = 0$, and so we only have to pay attention to the latter two terms of the above expression.

We now want to decompose our momentum operator $\mathbf{p}$ into its radial and angular parts, such that we can reduce the system to a one-dimensional problem. Our first instinct would be to define the radial angular momentum operator as $p_r = \mathbf{p} \cdot \mathbf{r}$, but this clearly does not work as this would make p_r manifestly not Hermitian. We thus adopt the alternative definition

$$p_r = \frac{1}{2}\left(\widehat{\mathbf{r}} \cdot \mathbf{p} + \mathbf{p} \cdot \widehat{\mathbf{r}}\right) = \frac{i\hbar}{2}\left(\frac{1}{r}\mathbf{r} \cdot \nabla + \nabla \cdot (r/\mathbf{r})\right) = -\frac{i\hbar}{2}\left(\frac{\partial}{\partial r} + \frac{3}{r} - \frac{r}{r^2} + \frac{\partial}{\partial r}\right) \tag{1.2}$$

Simplifying this, we obtain the expression

$$\boxed{p_r = -i\hbar\left(\frac{\partial}{\partial r} + \frac{1}{r}\right)} \tag{1.3}$$

Squaring up this expression:

$$p_r^2 = -\hbar^2\left(\frac{\partial^2}{\partial r^2} + \frac{2}{r}\frac{\partial}{\partial r} - \frac{1}{r^2} + \frac{1}{r^2}\right) = -\frac{\hbar^2}{r^2}\frac{\partial}{\partial r}\left(r^2\frac{\partial}{\partial r}\right) \tag{1.4}$$

We note how this is the radial part of the Laplacian in spherical polar coordinates. This means that we can decompose the momentum as

$$\frac{p^2}{2m} = \underbrace{\frac{p_r^2}{2m}}_{\text{Radial}} + \underbrace{\frac{L^2}{2mr^2}}_{\text{Angular}} \tag{1.5}$$

Our Hamiltonian thus becomes

$$H = \frac{p_r^2}{2\mu} + \frac{L^2}{2\mu r^2} - \frac{Ze^2}{4\pi\epsilon_0 r} \tag{1.6}$$

where we have introduced the Coulomb potential associated with a nucleus of charge Z. It follows that L^2 commutes with H as L^2 is spherically symmetric, and the remainder of the terms in H depend only on radius. Therefore, there exists a complete set of mutual eigenkets of H, L^2 and L_z, which we use to denote the states of hydrogenic atoms. We write this as $|n, \ell, m_\ell\rangle$, which can be thought of as a product state of $|n, \ell\rangle$ and $|\ell, m_\ell\rangle$. This means that we can automatically write that

$$\langle r, \theta, \phi | n, \ell, m_\ell\rangle = \underbrace{\langle r|n, \ell\rangle}_{\text{radial}} \underbrace{\langle \theta, \phi|\ell, m_\ell\rangle}_{\text{angular}} = R_{n\ell}(r)\, Y_\ell^{m_\ell}(\theta, \phi) \tag{1.7}$$

Substituting this trial solution into the TISE:

$$H \langle r, \theta, \phi|\psi\rangle = E \langle r, \theta, \phi|\psi\rangle \tag{1.8}$$

$$\left(H_r + \frac{L^2}{2\mu r^2}\right) RY = ERY \tag{1.9}$$

$$\underbrace{\frac{1}{Y} L^2\, Y}_{\text{function of } \theta, \phi \text{ only}} = \underbrace{2\mu r^2 \left(E - \frac{1}{R} HR\right)}_{\text{function of } r \text{ only}} \tag{1.10}$$

Evidently, as we know that the angular eigenfunctions are the spherical harmonics, we have an easy choice of separation constant. This means that the radial equation becomes

$$\left[-\frac{\hbar^2}{2\mu r}\frac{\partial^2}{\partial r^2} + \frac{\ell(\ell+1)\hbar^2}{2\mu r^2} - \frac{Ze^2}{4\pi\epsilon_0 r}\right] rR(r) = ErR(r) \tag{1.11}$$

The analytic solutions to the above equation are the radial eigenfunctions given by

$$R_{n\ell}(r) \propto r^\ell e^{-\frac{Zr}{na_\mu}} L_{n-\ell-1}^{2\ell+1}(r) \tag{1.12}$$

where $L_{n-\ell-1}^{2\ell+1}(r)$ are the Lageurre polynomials, and we have defined $a_\mu = \frac{m_e}{\mu} a_0$. Due to the definition of the the Laguerre polynomials, we require that the lower index is greater than or equal to zero, giving us the condition that $0 \le \ell \le n-1$. The corresponding energy eigenvalue is given by

$$\boxed{E_n = -\frac{1}{2}\mu(\alpha c)^2 \frac{Z^2}{n^2}} \tag{1.13}$$

where α is the *fine structure constant* ($\backsim 1/137$). Consequently, we define the Rydberg unit of energy $\mathcal{R}$ and the Rydberg constant R_∞ by

$$\mathcal{R} = hcR_\infty = \frac{1}{2} m_e(\alpha c)^2 = 13.6 \text{ eV} \tag{1.14}$$

The second definition is quite useful for cases involving transitions, as this allows us to convert quickly between energy and wave-number.

1.1.2 Radial wavefunctions

Evidently, one does not have to be able to recall all of the radial wave-functions, but it is worth remembering those of the groundstate and first excited state:

$$R_{10}(r) = 2\left(\frac{Z}{a_\mu}\right)^{3/2} e^{-\frac{Zr}{a_\mu}}, \quad R_{20}(r) = 2\left(\frac{Z}{2a_\mu}\right)^{3/2} \left(1 - \frac{Zr}{2a_\mu}\right) e^{-\frac{Zr}{2a_\mu}} \tag{1.15}$$

where again $a_\mu = \frac{m_e}{\mu} a_0$. Note that these functions have only been normalised over the interval $[0, \infty]$, rather than also over the angular parts of the distributions. From these functions, it is clear that the characteristic scale length for the system is na_μ/Z.

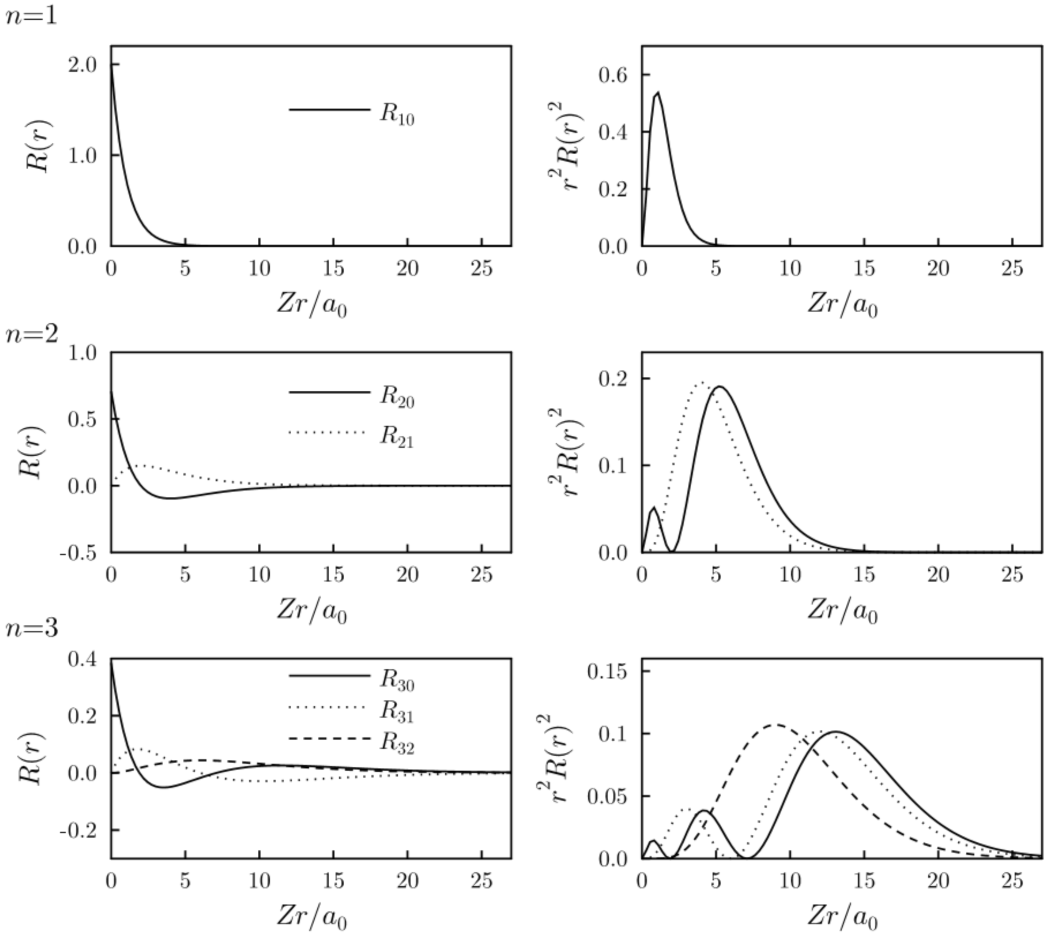

Figure 1.1: Graphs of some wavefunctions (left) and probability densities (right) for low values of n

A notable point about the groundstate (as well as all other $\ell = 0$ states) is that it has a non-vanishing probability of being near $r = 0$, as the Coulomb potential is unbounded near the origin, only held in check by the strong force. Some graphs of the lower order radial wavefunctions are shown in figure 1.1.

The plots in the left-hand column simply show the wavefunction, while those in the right-hand column show the probability of finding the electron in the range $[r, r+dr]$. There are $n-1$ nodes for each value of n, and so as you increase n, you will obtain more frequent, and sharper peaks. This means that for higher n, the electrons tend to be found in more and more discrete bands further away from the origin.

Size of Orbit

We can now calculate the expectation value $\langle r \rangle$ to give us an idea of the typical size of a 'circular' orbit. To do this, we assume that $\ell = n-1$, meaning that $L_0^{2\ell+1} = 1$. This gives us a much simpler radial wave-function of the form

$$R_{n,n-1}(r) \propto r^{n-1} e^{-\frac{Zr}{na_\mu}} \tag{1.16}$$

Then, the expectation value is calculated as

$$\langle r\rangle = \frac{\int_0^\infty dr\; r^2\,|\psi|^2 r}{\int_0^\infty dr\; r^2|\psi|^2} = \frac{\int_0^\infty dr\; r^{2n+1}e^{-2Zr/(na_\mu)}}{\int_0^\infty dr\; r^{2n}e^{-2Zr/(na_\mu)}} = \frac{na_\mu}{2}\frac{(2n+1)!}{(2n)!}$$

This means that our expression for our orbital size is

$$\boxed{\langle r\rangle = n\left(n+\frac{1}{2}\right)a_\mu} \tag{1.17}$$

Similarly, it can be shown that

$$\langle r^2\rangle = n^2\,(n+1)\left(n+\frac{1}{2}\right)a_\mu^2$$

This means that for large n, $\langle r\rangle \propto n^2$ while $\sigma_r \propto n^{3/2}$. This means that the variance around the average does not scale with the average, allowing the latter to tend towards a very sharp peak. In this limit, we recover the Bohr model for hydrogenic atoms.

1.1.3 A useful summary

A summary of the important results in this section is shown in the box below.

$$|n,\ell,m_\ell\rangle \quad \text{for} \quad \begin{cases} 1\le n \\ 0\le \ell\le n-1 \\ -\ell\le m_\ell\le \ell \end{cases} \tag{1.18}$$

$$p_r = -i\hbar\left(\frac{\partial}{\partial r}+\frac{1}{r}\right) \tag{1.19}$$

$$E_n = -\frac{1}{2}\mu(\alpha c)^2\frac{Z^2}{n^2} \tag{1.20}$$

$$\langle r\rangle = n\left(n+\frac{1}{2}\right)a_\mu \tag{1.21}$$

It is, to varying degrees of accuracy, often a good approximation to use hydrogenic formulae for different atoms - however relativistic effects start to become important for helium and anything more complex. What sort of fractional error would we expect when neglecting relativistic effects for hydrogen? We have that

$$E_{\text{ clas.}} = \frac{1}{2}\mu(\alpha c)^2\frac{Z^2}{n^2}$$
$$E_{\text{ rel.}} = \gamma mc^2$$

where γ is defined as normal in Special Relativity. The fractional error is given by

$$\frac{\delta E}{E_{\text{ rel.}}} = \frac{E_{\text{ rel.}}-E_{\text{ clas.}}}{E_{\text{ rel.}}} \backsim \frac{1}{2}\left(\frac{v}{c}\right)^2 \backsim \alpha^2 \backsim 10^{-4}$$

This means that the fractional error isn't particularly large when neglecting relativistic effects in hydrogen. However, it if we want to achieve a more accurate treatment of atomic structure for heavier elements (that is, elements with a higher Z), we will start having to take into account effects of this magnitude. That is, relativistic effects shall start to matter, as we will soon see.

1.2 An upgraded Hamiltonian

Evidently, the Hamiltonian that we adopted in the previous section was a greatly simplified model, designed to allow us to obtain analytical solutions to our system that we could use to interpret its macroscopic behaviour. We want to 'upgrade' our Hamiltonian to allow us to describe the behaviour of multiple electron atoms, as well as other internal interaction effects. With this in mind, let us adopt the following Hamiltonian for the remainder of these notes:

$$H_{\text{atomic}} = \underbrace{H_{CF}}_{\text{gross structure}} + \underbrace{\delta H_{RE} + \delta H_{SO}}_{\text{fine structure}} + \underbrace{\delta H_{HF}}_{\text{hyperfine structure}} \tag{1.22}$$

where each term corresponds to the following

- H_{CF} = Central Field Approximation
- δH_{RE} = Residual Electrostatic Interaction
- δH_{SO} = Spin Orbit Interaction
- δH_{HF} = Hyperfine Structure Interaction

From the notation above, it is clear that δH_{RE}, δH_{SO} and δH_{HF} are all perturbations on H_{CF}, but we have given no indication as to their ordering. In general, these elements of the Hamiltonian are ordered as:

$$\langle H_{CF}\rangle \gg \langle \delta H_{RE}\rangle , \langle \delta H_{SO}\rangle \gg \langle \delta H_{HF}\rangle \tag{1.23}$$

The ordering of the fine structure terms depends on the particular atom being considered, as well as other external factors. There are certain circumstances where this overall ordering breaks down - that is, where terms become comparable to one another, such that they are no longer perturbations - which we shall discuss where relevant.

Now that we have established our overall Hamiltonian, the plan is to investigate each of these Hamiltonians in turn. We shall examine the origin of each term, and investigate their effects on the overall energy levels and behaviour of the atomic system. This author will attempt to do so in a logical order, while preserving clarity as to which terms are actually being taken into account at each stage, in the hope that this will provide greater clarity over other notes available.

2. *The Hierarchy of Perturbations*

In this chapter, we will look at the various terms of our Hamiltonian H_{atomic}, treating the following:

- Gross Structure
- Fine Structure
- Hyperfine Structure
- Magnetic Field Effects

We shall see that the order of magnitude of these terms ranges from $\backsim$ a few eV in the case of gross structure, to $\backsim 10^{-6}$ eV in the case of hyperfine structure. We would thus expect each level of further perturbation to become harder to observe experimentally, which is indeed what we find in practise.

Some (potentially) useful integrals:

$$\begin{aligned}
\int_{-\infty}^{\infty} dx\; e^{-(b^2x^2+ax)} &= \frac{\sqrt{\pi}}{b} e^{a^2/4b^2} \\
\int_{0}^{\infty} dx\; x^n e^{-ax} &= \frac{n!}{a^{n+1}} \\
\int_{0}^{\infty} dx\; x^{2n+1} e^{-ax^2} &= \frac{1}{2}\frac{n!}{a^{n+1}} \\
\int_{0}^{\pi} d\theta\; \sin^{2\ell+1}\theta &= \frac{2(2^\ell \ell!)^2}{(2\ell+1)!}
\end{aligned}$$

2.1 Gross Structure

As anticipated in section 1.2, the Hamiltonian for a multiple particle system is significantly more complicated that that given by (1.1), as we have to take into account the interactions between each of the particles. Suppose that we index our N electrons by i. Then:

$$H_0 = \underbrace{\sum_i^N \left(-\frac{\hbar^2}{2\mu}\nabla_i^2 - \frac{Ze^2}{4\pi\epsilon_0 r_i}\right)}_{\text{interaction with nucleus}} + \underbrace{\sum_{i>j}^N \frac{e^2}{4\pi\epsilon_0 r_{ij}}}_{\text{inter particle interactions}} \tag{2.1}$$

The last term in this equation prevents the TISE from being separable into the N single particle equations, and is too large an effect to solve as a perturbation. An effective solution to this problem is to use the *Central Field approximation.*

2.1.1 The Central Field Approximation

We recognise that a large component of the force between electrons will be directed radially inwards, as the electrons will be located at different radii due to a combination of the Pauli exclusion principle and other effects. Given this, we decompose H_0 using a central field $U(r)$:

$$H_0 = H_{CF} + \delta H_{RE} \tag{2.2}$$

where

$$H_{CF} = \sum_i^N \left(-\frac{\hbar^2}{2\mu}\nabla_i^2 + U(r_i)\right) \tag{2.3}$$

$$\delta H_{RE} = \sum_{i>j}^N \frac{e^2}{4\pi\epsilon_0 r_{ij}} - \sum_i^N \left(\frac{Ze^2}{4\pi\epsilon_0 r_i} + U(r_i)\right) \tag{2.4}$$

Note that this decomposition is identical to our original expression for H_0, except now we have separated it into a spherically symmetric, separable term H_{CF}, and a 'compensating' term δH_{RE} that we can treat by perturbation methods (see section 2.2.1). The advantage of using this central field approximation is that we once again obtain a Hamiltonian that commutes with L^2 and L_z, meaning that we can continue to use our hydrogenic states $|n, \ell, m_\ell\rangle$ (where again n, ℓ and m_ℓ are single electron quantum numbers). The radial wave equation is simply (1.11), but with the Coulomb potential replaced by $U(r)$. We would thus expect $\langle H_{CF}\rangle \backsim$ eV.

What form does out central field potential $U(r)$ take? We can get a rough idea of it's form by considering asymptotic limits. For an electron far from the nucleus, the other inner electrons screen it from the effect of the nuclear charge Z, such that it sees an *effective nuclear charge* $Z_{eff} \backsim 1$. Conversely, when it is close to the nucleus, we would expect that it experiences the full nuclear charge of Z. By analogy to the nuclear interaction term of (2.1), we adopt a potential of the form:

$$\boxed{U(r) = -Z_{eff}(r)\frac{e^2}{4\pi\epsilon_0 r}} \tag{2.5}$$

where $Z_{eff}(r)$ is some function satisfying the conditions that $Z_{eff}(r \to 0) = Z$ and $Z_{eff}(r \to \infty) \backsim 1$; an approximate form of this is shown in figure 2.1. Generally, states with higher n and ℓ will approximate hydrogenic solutions, as these occur in the region

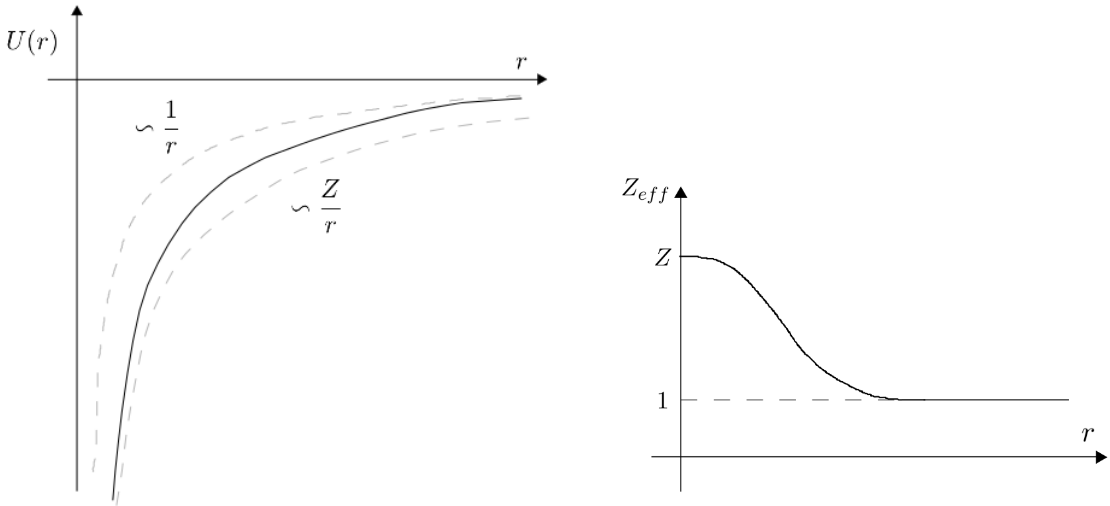

(a) (b)

Figure 2.1: (a) An approximate form of the central potential $U(r)$ (b) An approximate form for the effective charge Z_{eff}

where $U(r) \backsim 1/r$.

Finding $U(r)$ exactly is a task for recursive numerical methods, such as the Hartee method. This involves the following steps:

1. Guess a form of the potential $U(r)$
2. Solve for the single electron wavefunctions $\phi_i(\mathbf{r})$
3. Find the charge density $\rho(\mathbf{r}) = -\sum_i e\,|\phi_i(\mathbf{r})|^2$
4. Find the resultant potential $U(r)'$ from the electric field $\mathbf{E}$

One can then iterate steps 2 to 4 until a self-consistent solution is found. This can be extended further by the Hartee-Fock method, which includes the effects of Pauli exclusion principle in the algorithm. As a result, it generates a central potential that gives rise to fully anti-symmetrised spatial wavefunctions.

2.1.2 Electronic Configurations

Each electron within an multiple electron atom has a particular n and ℓ associated with it; m_ℓ makes no contribution to the energy. Electronic configurations are a way of specifying these quantum numbers, notated as below.

The values of ℓ are denoted using spectroscopic notation. That is, we used the letters $s, p, d, f, \dots$ to refer to $\ell = 0, 1, 2, 3, \dots$ and so on. There is no particular logic behind why this is the case; it is simply a notational convention, and one that has to be learnt.

Each *energy orbital* is degenerate in n and ℓ; there are $2n^2$ states for each value of n (a consequence of Pauli exclusion), and $2(2\ell + 1)$ for each value of ℓ_i (factor of two due to spin degeneracy). It is important to remember that $0 \leq \ell_i \leq n$, and that the sum of the number of electrons in all of the orbitals is equal to the atomic number Z (in the case of

Number of electrons in orbital. Maximum at $2(2\ell+1)$

Value of ℓ for orbital

Energy Orbital

$$n_i\ell_i^{\#}\ldots n_j\ell_j^{\#}$$

Principal quantum number

Figure 2.2: Notation for electronic configurations

neutral atoms). These can be useful consistency checks when constructing configurations.

The energy orbitals with the lowest energy will fill up first, and for all elements up for Argon (Ar), this corresponds to the orbitals with the lowest n. After Ar, we find that

$$\begin{aligned}
\text{Ar}:&1s^2 2s^2 2p^6 3s^2 3p^6 \\
\text{K}:&1s^2 2s^2 2p^6 3s^2 3p^6 \quad 4s \\
\text{Ca}:&1s^2 2s^2 2p^6 3s^2 3p^6 \quad 4s^2 \\
\text{Sc}:&1s^2 2s^2 2p^6 3s^2 3p^6 3d\, 4s^2
\end{aligned}$$

and so on. Logically, we would expect the next orbital to be filled in Potassium (K) to be the $3d$ orbital. However, the fact that it has $\ell = 2$ means that - on average - the electron is localised further away from the nucleus, and so is partially screened from the nuclear charge. This causes it to be higher in energy than the $4s$ state, an so it does not fill up next. For higher elements, the states become significantly more complicated to deduce, though it is not particularly crucial to be able to write down their electronic configurations; rather, one should be able to extract information from a given electronic configuration.

We note that full orbitals make no contribution to the overall angular momentum; this is because they must have spherically symmetric electrostatic potentials, forcing $\ell = 0$ (spherically symmetric states cannot have a non-zero value of ℓ, as to do so would define a special spatial direction, creating a contradiction).

2.1.3 Alkali Atoms

The Akali metals are found in the first group of the periodic table, and have a single valence electron that is responsible for all the system dynamics. As the electron core consists of full shells, it makes no contribution to ℓ and s, as above. For example, consider Sodium (Na, $Z = 11$):

$$\text{Na}: \underbrace{1s^2 2s^2 2p^6}_{\text{core}} \quad \underbrace{n\ell}_{\text{valence electron}} \tag{2.6}$$

The core has the same electronic configuration as Neon (Ne), and one will often see the configuration in the first bracket simply replaced by '[Ne]' in shorthand notation. This makes it explicit that Na is simply a Ne electron core with an extra valence electron.

This valence electron thus moves in a hydrogenic potential, as it is shielded by the inner electrons most of the time. This means that for large ℓ, we can write that $Z_{eff} \backsim Z - (Z - 1) = 1$. However, this approximation begins to break down for lower ℓ, as the electron has a higher probability of being found in locations close to the nucleus. We take account of this by the *quantum defect* δ

$$\boxed{E_{n,\ell} = -\frac{1}{2}\mu(\alpha c)^2\frac{1}{n^{*2}}, \quad n^* = n - \delta(\ell)} \tag{2.7}$$

We expect that as $\ell \to \infty$, the akali energy levels approach those of the hydrogenic energy levels: $n^* \to n$ and so $\delta \to 0$. This means that δ must be some function of ℓ; that is, $\delta = \delta(\ell)$. In practise, there is some dependence of δ on n, but it is so small that we can effectively ignore it. The values for δ are determined empirically by measuring the energy difference between the observed energy levels, and the ideal hydrogenic energy levels. For Na, we find that $\delta(s) \backsim 1.34$, $\delta(p) \backsim 0.88$ and $\delta(d) \backsim 0$. Evidently, these corrections are going to be different for other elements.

Write down the groundstate configuration for Na. Find the quantum defect of this level, given that the first ionisation potential of sodium is 5.14 eV.

From (2.6), we already know the electronic configuration corresponding to the full orbitals. Then, the groundstate will have $n = 3$, and $\ell = 0$. Thus, we write that

$$\text{Na} : 1s^2 2s^2 2p^6 3s \tag{2.8}$$

Then, we can write that

$$5.14 \text{ eV} = \frac{\mathcal{R}}{n^{*2}} = \frac{13.6 \text{ eV}}{n^{*2}} \quad \longrightarrow \quad n^* \backsim 1.63 \tag{2.9}$$

We know that we are in the $3s$ state.

$$n^* = n - \delta(s) = 3 - \delta(s) \quad \longrightarrow \quad \delta(s) \backsim 1.37 \tag{2.10}$$

Note that the question refers to the first ionisation potential; this is the amount of energy required to liberate the first electron from the atom. In the case of akali atoms, this will simply give the energy of the groundstate of the valence electron.

2.2 Fine Structure

We are now going to move on to a consideration of perturbation effects on our base Hamiltonian H_{CF}. These effects will have smaller energy overall than the gross structure energy, but these fine structure effects are still easily observable experimentally. It must be stressed that while we assume that

$$\langle H_{CF}\rangle \gg \langle \delta H_{RE}\rangle , \langle \delta H_{SO}\rangle \tag{2.11}$$

we make no assumption concerning the ordering of the right hand two terms, which depends on other factors to be discussed in section 2.2.3.

2.2.1 Residual Electrostatic Interaction

Apart from when constructing configurations, we have thus far neglected the effect of spin on the energy of the atom. This would have been fine if we were just considering hydrogenic atoms, but in the case of more than one electron, the spin state of the system does start to effect the energy. This is known as the residual electrostatic interaction.

Exchange Symmetry

Suppose that we can specify the state of our system by the state $|a_1, a_2, a_3, \dots\rangle$. Define the exchange operation

$$|a_1, a_3, a_2, \dots\rangle = e^{i\phi} |a_1, a_2, a_3, \dots\rangle \tag{2.12}$$

where the complex phase ϕ results from swapping two of the coordinates a_i. Suppose that we perform the operation a second time:

$$|a_1, a_2, a_3, \dots\rangle = e^{2i\phi} |a_1, a_2, a_3, \dots\rangle \quad \longrightarrow \quad e^{2i\phi} = 1,\ e^{i\phi} = \pm 1 \tag{2.13}$$

This means that there are two types of exchange symmetry; symmetric (corresponding to bosons) and antisymmetric (corresponding to fermions). As electrons are fermions, means that we must either have a symmetric spatial state and antisymmetric spin state, or an antisymmetric spatial state and symmetric spin state.

Suppose that we are considering an atom with only two valence electrons, allowing us to characterise the system using the following product state

$$|\psi\rangle = |n_1, \ell_1, n_2, \ell_2, m_{s1}, m_{s2}\rangle = \underbrace{|n_1, \ell_1, n_2, \ell_2\rangle}_{\text{spatial}} \underbrace{|m_{s1}, m_{s2}\rangle}_{\text{spin}} \tag{2.14}$$

Let the single-particle wavefunctions for the two electrons be $\phi_1(\mathbf{x}_1)$ and $\phi_2(\mathbf{x}_2)$. The possibilities for the spatial wavefunction are thus given by

$$\langle \mathbf{x}_1, \mathbf{x}_2 | n_1, \ell_1, n_2, \ell_2\rangle = \begin{cases} \frac{1}{\sqrt{2}} [\phi_1(\mathbf{x}_1)\phi_2(\mathbf{x}_2) + \phi_2(\mathbf{x}_1)\phi_1(\mathbf{x}_2)] & \text{symmetric} \\ \frac{1}{\sqrt{2}} [\phi_1(\mathbf{x}_1)\phi_2(\mathbf{x}_2) - \phi_2(\mathbf{x}_1)\phi_1(\mathbf{x}_2)] & \text{antisymmetric} \end{cases} \tag{2.15}$$

Similarly, the possibilities for the spin wavefunctions are given by

$$|m_{s1}, m_{s2}\rangle = \begin{cases} |1, 1\rangle & \\ |-1, -1\rangle & \text{symmetric (triplet)} \\ \frac{1}{\sqrt{2}} (|1, -1\rangle + |-1, 1\rangle) & \\ & \\ \frac{1}{\sqrt{2}} (|1, -1\rangle - |-1, 1\rangle) & \text{antisymmetric (singlet)} \end{cases} \tag{2.16}$$

Exchange Interaction

Conveniently, the wavefunctions given by (2.15) form a diagonal basis for the Hamiltonian δH_{RE}, as they are no longer (energy) degenerate. This means that the energy shift is given by

$$\delta E_{RE} = \langle n_1, \ell_1, n_2, \ell_2 | \, \delta H_{RE} \, | n_1, \ell_1, n_2, \ell_2 \rangle = J \pm K \tag{2.17}$$

where the integrals J and K are given by

$$J = \int d^3\mathbf{x}_1 d^3\mathbf{x}_2 \; |\phi_1(\mathbf{x}_1)\phi_2(\mathbf{x}_2)|^2 \; \delta H_{RE} \tag{2.18}$$

$$K = \int d^3\mathbf{x}_1 d^3\mathbf{x}_2 \; \phi_1^*(\mathbf{x}_1)\phi_2^*(\mathbf{x}_2)\phi_2(\mathbf{x}_1)\phi_1(\mathbf{x}_2) \, \delta H_{RE} \tag{2.19}$$

The positive sign in (2.17) corresponds to the symmetric spatial wavefunction, while the negative sign corresponds to the antisymmetric spatial wavefunction, meaning that there is an energy difference of $2K$ between these states. Thus, the singlet state is higher in energy than the triplet state. This effect is often referred to as *singlet-triple splitting*.

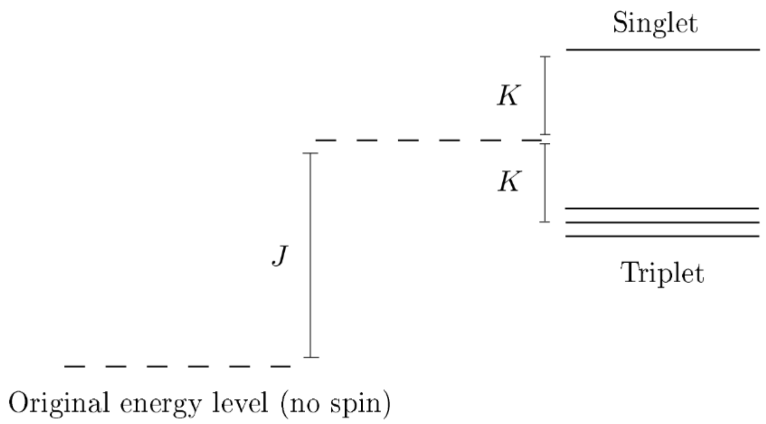

Figure 2.3: A schematic of singlet-triplet splitting

It is clear that the energy of the system now depends on the angular momentum and the spin state of the system, as well as the original configuration. This means that for a more general case, we adopt states of the form

$$|L, M_L, S, M_S\rangle \tag{2.20}$$

where L and S are the quantum numbers corresponding to the operators $\mathbf{L} = \sum_i \mathbf{L}_i$ and $\mathbf{S} = \sum_i \mathbf{S}_i$; that is, they denote the total angular momentum and spin of the system.

As a result, we now need to modify our spectroscopic notation to add this new information about the state of our system. This is shown in figure 2.4. ^{2S+1}L is known as a *term* that is used to specify these extra quantum numbers that influence the energy of the system, which we write after the electronic configuration. Once again, the value of L is indicated using $S, P, D, F, \ldots$ (note the capitals). The ℓ_i and ℓ_j refer to the angular momentum of particular orbitals. This is shown in figure 2.4.

$$\underbrace{n_i\ell_i^{\#}\dots n_j\ell_j^{\#}}_{\text{Configuration}}\;{}^{\overset{\text{Total spin}}{2S+1}}\underset{\text{Value of (total) }L}{L}$$

Figure 2.4: Spectroscopic notation of the electronic configuration and terms

2.2.2 Spin Orbit Interaction

The next fine structure effect that we are going to examine is that of the *spin-orbit* (SO) *interaction.* This is a relativistic correction to the energy that arises due to the fact that the electron is moving through an attractive potential $U(r)$, as per the central field approximation. As this is a magnetic effect, we need to first derive the dipole moment due to the momentum associated with an electron.

Magnetic dipole moment

An important quantity in such calculations is the *Bohr magneton*, that we define as

$$\boxed{\mu_B = \frac{e\hbar}{2m_e}} \tag{2.21}$$

Now, consider an electron with orbital angular momentum $\mathbf{L}_i$ and spin angular momentum $\mathbf{S}_i$, in a magnetic field described by the magnetic potential $\mathbf{A}$. This will have Hamiltonian

$$H_{\mathbf{A}} = \frac{1}{2m_e}(\mathbf{p}_i - q\mathbf{A})^2 + U(r) = \underbrace{\frac{\mathbf{p}_i^2}{2m_e} + U(r)}_{H_{CF}} - \frac{1}{2m_e}(2q\,\mathbf{p}_i\cdot\mathbf{A} - q^2\mathbf{A}\cdot\mathbf{A}) \tag{2.22}$$

Assume that the magnetic field is weak, such that $q^2\mathbf{A}^2/2m_e \ll H_{CF}$, meaning that we can neglect terms of $\mathcal{O}(\mathbf{A}^2)$ and above:

$$H_{\mathbf{A}} \backsim H_{CF} - \frac{q}{m_e}\mathbf{p}_i\cdot\mathbf{A} \tag{2.23}$$

We shall consider the magnetic field to be uniform, as it is very difficult to create a field that has significant spatial variation over the lengthscale of the atom. This means that a convenient choice of $\mathbf{A}$ is

$$\mathbf{A} = \frac{1}{2}\,\mathbf{B}\times\mathbf{r} \tag{2.24}$$

The extra term in the Hamiltonian thus becomes

$$-\frac{q}{2m_e}\mathbf{p}_i\cdot(\mathbf{B}\times\mathbf{r}) = -\frac{q}{2m_e}\mathbf{B}\cdot(\mathbf{r}\times\mathbf{p}_i) = -\frac{\mu_B}{\hbar}\mathbf{L}_i\cdot\mathbf{B} \tag{2.25}$$

This means that the electron has an orbital angular momentum magnetic moment of

$$\boldsymbol{\mu}_{L_i} = -\frac{\mu_B}{\hbar}\mathbf{L}_i \tag{2.26}$$

Similarly, the intrinsic electron spin also gives rise to a magnetic dipole moment:

$$\boldsymbol{\mu}_{S_i} = -\frac{\mu_B}{\hbar}g_s\mathbf{S}_i \tag{2.27}$$

We note that $g_s \backsim 2$ for an electron. This means that the total dipole moment for a single electron in a magnetic field is given by

$$\boldsymbol{\mu}_i = -\frac{\mu_B}{\hbar}(\mathbf{L}_i + g_s\mathbf{S}_i) \tag{2.28}$$

For multiple electron system, the total magnetic moment is simply given by $\boldsymbol{\mu} = \sum_i \boldsymbol{\mu}_i$. Noting once again that $\mathbf{L} = \sum_i L_i$ and $\mathbf{S} = \sum_i \mathbf{S}_i$, it follows that the magnetic moment of such as system is given by

$$\boxed{\boldsymbol{\mu} = -\frac{\mu_B}{\hbar}(\mathbf{L} + g_s\mathbf{S})} \tag{2.29}$$

Generally, one does not need to derive this quantity when considering magnetic interactions in atoms, but it is useful to know where it comes from quantum mechanically (as it's quite simple to show classically).

SO in single electron atoms

Let us initially consider the simple case of hydrogenic atoms for which $\mathbf{L} = \mathbf{L}_i$, $\mathbf{S} = \mathbf{S}_i$ and $\mathbf{p} = \mathbf{p}_i$. We know from relativistic electrodynamics that in the rest frame of the electron, a magnetic field results from the central field $U(r)$:

$$\mathbf{B}_{\text{internal}} \equiv \mathbf{B} = -\frac{1}{c^2}(\mathbf{v} \times \mathbf{E}) = -\frac{1}{c^2}(\mathbf{v} \times (-\nabla U)) \tag{2.30}$$

The SO Hamiltonian is then given by

$$\boxed{\delta H_{SO} = -\frac{1}{2}\,\boldsymbol{\mu} \cdot \mathbf{B}} \tag{2.31}$$

The factor of a half comes from *Thomas Procession*, a relativistic correction to the spin of a particle (see B2 notes), though it is not always necessary to include it in the calculation. Introducing our expression for $\boldsymbol{\mu}$, we find that:

$$\delta H_{SO} = \frac{g_s\mu_B}{2\hbar c^2}\mathbf{S} \cdot (\mathbf{v} \times \nabla U) = \frac{g_s\mu_B}{2\hbar m_e c^2}\mathbf{S} \cdot \left(\mathbf{p} \times \frac{\hat{\mathbf{r}}}{r}\frac{\partial U}{\partial r}\right) = \frac{g_s\mu_B}{2\hbar m_e c^2}\frac{1}{r}\frac{\partial U}{\partial r}\mathbf{S} \cdot \mathbf{L} \tag{2.32}$$

where we have ignored the orbital angular momentum contribution to $\boldsymbol{\mu}$ (as we are in the rest frame of the electron) and observed that $\mathbf{L} = \mathbf{r} \times \mathbf{p}$. We now assume that the central potential takes the form

$$U(r) = -\frac{Ze}{4\pi\epsilon_0 r} \tag{2.33}$$

allowing us to arrive at the final expression for the Hamiltonian of

$$\delta H_{SO} = \frac{Ze^2}{8\pi\epsilon_0 m_e^2 c^2}\,\mathbf{S} \cdot \mathbf{L}\,\frac{1}{r^3} \tag{2.34}$$

Evidently, both J^2 and J_z are constants of the motion, meaning that they must commute both with the unperturbed Hamiltonian, and δH_{SO}, as are L^2 and S^2. This means that we can use the basis labelled by the kets $|j, m_j, \ell, s\rangle$ (as we are dealing with a single valence electron). We need to consider the expectation values of $1/r^3$ and $\mathbf{S} \cdot \mathbf{L}$. For a hydrogenic atom with nucleic charge Z, the first of these is:

$$\left\langle \frac{1}{r^3} \right\rangle = \frac{2}{\ell(\ell+1)(2\ell+1)}\frac{Z^3}{(na_\mu)^3}$$

We would expect an expression of this form as the smaller the system size, the greater the kinetic energy (and thus angular momentum), meaning that the spin-orbit interaction will increase in magnitude. The second can be calculated by recognising that

$$\mathbf{S}\cdot\mathbf{L} = \frac{1}{2}(J^2 - L^2 - S^2) \tag{2.35}$$

Then

$$\langle\mathbf{S}\cdot\mathbf{L}\rangle = \frac{1}{2}\left\langle J^2 - L^2 - S^2\right\rangle = \frac{1}{2}\left[j(j+1) - \ell(\ell+1) - s(s+1)\right]\hbar^2 \tag{2.36}$$

Putting all of this together, and re-writing the numerical pre-factor in δH_{SO}, the first order changes in the energy are given by

$$\boxed{\delta E_{SO} = \frac{\beta_{n,\ell}}{2}(j(j+1) - \ell(\ell+1) - s(s+1))\hbar^2} \tag{2.37}$$

The factor

$$\beta_{n,\ell} = \frac{1}{2}mc^2(\alpha Z)^4\left(\frac{\mu}{nm_e}\right)^3\frac{1}{\ell(\ell+1)(\ell+1/2)} \tag{2.38}$$

is a parameter that specifies the strength of the perturbation. For a general hydrogenic level, we have that $j_\pm = \ell \pm 1/2$. The 'spin-up' states are shifted by an amount

$$\delta E_+ \propto j_+(j_+ + 1) - \ell(\ell+1) - \frac{3}{4} = \left(\ell + \frac{1}{2}\right)\left(\ell + \frac{3}{2}\right) - \ell(\ell+1) - \frac{3}{4} = \ell \tag{2.39}$$

Likewise, the 'spin-down' states are shifted by an amount

$$\delta E_- \propto j_-(j_- + 1) - \ell(\ell+1) - \frac{3}{4} = \left(\ell - \frac{1}{2}\right)\left(\ell + \frac{1}{2}\right) - \ell(\ell+1) - \frac{3}{4} = -(\ell+1) \tag{2.40}$$

For each value of j, the spin-orbit interaction creates another $2j+1$ energy levels (due to degeneracy), and so the mean energy shift for the system is proportional to

$$\delta\bar{E}_{SO} \propto (2j_+ + 1)\delta E_+ + (2j_- + 1)\delta E_- = 0 \tag{2.41}$$

Thus, the mean energy shift for a system under the spin-orbit interaction is zero. This makes sense in the context of energy conservation; as the spin-orbit interaction is created by motion within the system, it cannot raise the mean energy of the system. Note that for akali atoms, we replace Z^4 with Z^2 as the effective charge of the system is reduced in comparison to the purely hydrogenic case.

As with the residual electrostatic interaction, we now need to add to our spectroscopic notation to include this new information about our system.

$$\underbrace{n_i\ell_i^{\#}\dots n_j\ell_j^{\#}}_{\text{Configuration}}\;\overbrace{{}^{2S+1}L}^{\text{Term}}{}_J$$

Total angular momentum

Figure 2.5: Spectroscopic notation of electronic configuration, terms and levels.

This addition is known as the *level* of the system. We thus have the *electronic configuration*, *terms*, and finally, *levels*. With this, we have completely specified the relevant quantum numbers L, S and J from which we can deduce the gross structure and fine structure energy levels for our system.

Hund's Rules

Now that have the full set of quantum numbers of our system, we need some way of calculating the relative energies between various configurations, terms and levels. For the groundstate, we can do this using Hund's Rules, named after the German physicist Friedrich Hund who formulated these rules around 1927. These are as follows:

- For a given electron configuration, the term with the maximum value of S has the lowest energy
- For a given value of S, the term with the largest value of L has the lowest energy
- For a given term, in an atom with the outermost shell half-filled or less, the level with the lowest value of J has the lowest energy. If the outermost shell is more than half-filled, the level with the highest J is lowest in energy

This means that, given a particular set of energy levels, it is possible to calculate the energy term corresponding to the ground state. Also helpful is the consideration that triplet states are, for most atoms, lower in energy than singlet states. These rules are simply a consequence of the fact that the system must obey Pauli exclusion; this means that only certain combinations of J, L and S are allowed for a given energy.

SO in multiple electron atoms

In the previous section, we simply considered the effect of spin-orbit coupling on a single electron. We are now going to suppose that we have multiple electrons that are indexed by i. Then, by analogy to (2.34), we can write that

$$\delta H_{SO} = \sum_i \zeta(r_i)\, \boldsymbol{\ell}_i \cdot \mathbf{s}_i \tag{2.42}$$

where $\zeta(r_i)$ is some function of the individual particle coordinates r_i. In this case, we adopt the basis $|J, M_J, L, S\rangle$. This means that ℓ and s are no longer good quantum numbers; we thus want to find the projections of $\boldsymbol{\ell}_i$ and $\mathbf{s}_i$ onto $\mathbf{L}$ and $\mathbf{S}$. We thus write

$$\delta E_{SO} = \sum_i \langle \zeta(r_i) \rangle \left\langle \frac{\langle \mathbf{s}_i \cdot \mathbf{S} \rangle}{S(S+1)} \mathbf{S} \cdot \frac{\langle \boldsymbol{\ell}_i \cdot \mathbf{L} \rangle}{L(L+1)} \mathbf{L} \right\rangle = \sum_i \langle \zeta'(r_i) \rangle \langle \mathbf{S} \cdot \mathbf{L} \rangle = \beta_{n,\ell} \, \langle \mathbf{S} \cdot \mathbf{L} \rangle \tag{2.43}$$

Unlike in the hydrogenic case, the coefficient $\beta_{n,\ell}$ is quite hard to calculate, meaning that we are often only interested in the dependence of the energy shifts on the quantum number J. As L and S are constant for a given J, we can write that

$$\Delta E_{J,J-1} = \delta E_{SO}(J) - \delta E_{SO}(J-1) \propto J(J+1) - J(J-1) \propto J \tag{2.44}$$

That is, the energy level splitting between two levels is proportional the J corresponding to the upper level. This is known as the *interval rule* for the SO interaction.

2.2.3 Coupling Schemes

In multiple particle systems, it is often the case that the angular momenta of the individual particles remain constants of the motion; it is usually some combination of the angular momenta that remains a constant of the motion. There are multiple ways in which one can combine the momenta, which gives rise to the so-called coupling schemes, which we shall detail below. It is always worth specifying the relevant coupling scheme that you are using when tackling a particular problem to ensure clarity for both yourself and the reader.

LS Coupling

We have implicitly assumed over the past few sections that we are working in the LS coupling scheme; that is, we have assumed that individual angular momenta combine as

$$\mathbf{L} = \sum_i \boldsymbol{\ell}_i, \quad L = |\ell_1 - \ell_2|, \ldots, \ell_1 + \ell_2 \tag{2.45}$$

$$\mathbf{S} = \sum_i \mathbf{s}_i, \quad S = |s_1 - s_2|, \ldots, s_1 + s_2 \tag{2.46}$$

$$\mathbf{J} = \mathbf{L} + \mathbf{S}, \quad J = |L - S|, \ldots, L + S \tag{2.47}$$

Note that the second column shows how the eigenvalues combine in the case of two particle systems. We can think of this in terms of the *vector model*, as shown in figure 2.6. Both $\mathbf{L}$ and $\mathbf{S}$ couple together and process around the axis defined by $\mathbf{J}$. It is thus clear why J, M_J, L and S are the good quantum numbers for our system, as supposed to M_L and M_S; the latter no longer have a well-defined direction. This is the reason why we had to find the projections of $\boldsymbol{\ell}_i$ and $\mathbf{s}_i$ onto $\mathbf{L}$ and $\mathbf{S}$ when evaluating (2.43).

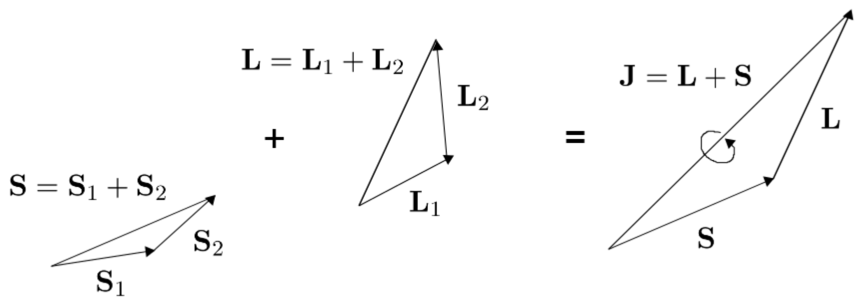

Figure 2.6: The vector model in LS coupling

The vector model is evidently just a way of representing the angular momentum coupling, and is not what actually occurs; it is a classical way of visualising quantum mechanical effects. One tutor of this author once described explaining the vector model as "getting my special tin of bullshit out, and applying liberally".

JJ Coupling

Under the LS coupling scheme, the fine structure perturbations are ordered as

$$\langle \delta H_{RE} \rangle \gg \langle \delta H_{SO} \rangle \tag{2.48}$$

However, we note that $\langle \delta H_{RE} \rangle \propto Z$, where as $\langle \delta H_{SO} \rangle \propto Z^4$. This means that as Z increases, the magnitude of these perturbations will become comparable, and this ordering breaks down ($Z \backsim 30$). We then enter the regime of JJ coupling, where the angular momentum combines as

$$\mathbf{j}_i = \boldsymbol{\ell}_i + \mathbf{s}_i, \quad j_i = |\ell_i - s_i|, \ldots, \ell_i + s_i \tag{2.49}$$

$$\mathbf{J} = \sum \mathbf{j}_i, \quad J = |j_1 - j_2|, \ldots, j_1 + j_2 \tag{2.50}$$

This is because the spin-orbit coupling of the individual electrons to the nucleus is dominant, and so their angular momenta becomes conserved components of the motion. Under this coupling scheme, the order of the perturbations is reversed, namely:

$$\langle \delta H_{SO} \rangle \gg \langle \delta H_{RE} \rangle \tag{2.51}$$

2.3 Hyperfine Structure

Thus far in our calculations, we have implicitly assumed that the nucleus is a point like object with no spin angular momentum. We shall now investigate the effect of relaxing each of these assumptions, giving rise to *hyperfine structure* effects.

2.3.1 Finite size of the nucleus

Let us model the nucleus as a uniformly charged sphere of radius $R \backsim 10^{-15}$. This is a relatively good approximation, given that the spatial variation of fields related to the charge cannot vary greatly on the scale of R. Assume that the atom in question is hydrogenic. We can then describe the potential outside the nucleus as

$$U(r > R) = -\frac{Ze^2}{4\pi\epsilon_0 r} \tag{2.52}$$

The potential inside the sphere describing the nucleus is found using techniques from classical electromagnetism:

$$U(r < R) = -\int_{\infty}^{R} dr\, \frac{Ze^2}{4\pi\epsilon_0}\frac{1}{r^2} - \int_{R}^{r} dr\, \frac{Ze^2}{4\pi\epsilon_0}\frac{r}{R^3} = -\frac{Ze^2}{8\pi\epsilon_0 R}\left(3 - \frac{r^2}{R^2}\right) \tag{2.53}$$

This means that the perturbation acts only for $0 < r < R$ and is given by

$$\delta H_p = U(r < R) - U(r > R) = \frac{Ze^2}{8\pi\epsilon_0 R}\left(\frac{r^2}{R^2} - 3 + \frac{2R}{r}\right) \tag{2.54}$$

Assume that the atom in question is in the groundstate, meaning that we can use the first expression in (1.12) to calculate the shift according to first order perturbation theory:

$$\delta E_p = \frac{Ze^2}{2\pi\epsilon_0 R}\left(\frac{Z}{a_\mu}\right)^3 \int_0^R dr\, r^2 \left(\frac{r^2}{R^2} - 3 + \frac{2R}{r}\right) e^{-2Zr/a_\mu} \tag{2.55}$$

We know that $R/a_\mu \backsim 10^4 \ll 1$. This means that over the range of our integral, we can approximate that $e^{-2Zr/a_\mu} \backsim 1$.

$$\delta E_p \backsim \frac{Ze^2}{2\pi\epsilon_0 R}\left(\frac{Z}{a_\mu}\right)^3 \int_0^R dr\, r^2 \left(\frac{r^2}{R^2} - 3 + \frac{2R}{r}\right) \backsim \frac{Ze^2}{2\pi\epsilon_0 a_\mu}\frac{Z^3}{5}\left(\frac{R}{a_\mu}\right)^2 \tag{2.56}$$

The associated groundstate energy is given by

$$|E_1| = \frac{Z^2 e^2}{8\pi\epsilon_0 a_\mu} \tag{2.57}$$

This means that we can write the first order change in the energy as

$$\delta E_p = \frac{4}{5}|E_1|\left(\frac{ZR}{a_\mu}\right)^2 \tag{2.58}$$

Evidently, due to the fact that $R/a_\mu \backsim 10^{-4}$, this correction is vanishingly small in comparison to both fine structure and hyperfine structure effects. We could have also calculated the relative magnitude of the shift from simple scaling arguments:

$$\frac{\delta E_p}{|E_n|} \backsim \frac{\text{inner scale length}^2}{\text{outer scale length}^2} \backsim \frac{R^2}{(na_\mu/Z)^2} \backsim \left(\frac{ZR}{a_\mu}\right)^2 \tag{2.59}$$

2.3.2 Nuclear spin Interaction

Let the operator $\mathbf{I}$ be the operator corresponding to the spin angular momentum of the nucleus, which can take half integer values $I = 0, \frac{1}{2}, 1, \frac{3}{2}, \dots$. This has associated magnetic dipole moment

$$\boxed{\boldsymbol{\mu}_I = g_I \frac{\mu_N}{\hbar}\mathbf{I}} \tag{2.60}$$

This results in a shift in energy due to interaction with the magnetic field of the electrons. We define the nuclear magneton as

$$\mu_N = \mu_B \frac{m_e}{m_p} \tag{2.61}$$

Note the ratio of m_e/m_p; this means that the magnitude of the shift is reduced by a factor of 10^{-3} in comparison to the spin-orbit interaction. Suppose that the orbiting electrons create a magnetic field $\mathbf{B}_e$. Then the Hamiltonian of this perturbation is

$$\delta H_{HF} = -\boldsymbol{\mu}_I \cdot \mathbf{B}_e \tag{2.62}$$

Now, the contribution to the magnetic field $\mathbf{B}_e$ that the nucleus experiences is going to be dominated by s-electrons ($\ell = 0$), as these spend a greater amount of time close to the origin. As such, we shall ignore the contribution made by other electrons (though of course, it is still there). Let $\psi_{n,\ell}(r) = \langle r, \theta, \phi | n, \ell, m\rangle$. The s-electrons have a magnetic moment given by (2.29) with $\mathbf{L} = 0$, such that the magnetisation is given by

$$\mathbf{M} = -g_s \frac{\mu_B}{\hbar}\mathbf{S}\,|\psi_{n,\ell}(r)|^2 \tag{2.63}$$

We treat the distribution around $r = 0$ as being spherical, which gives the resultant magnetic field of

$$\mathbf{B}_e = \frac{2}{3}\mu_0 \mathbf{M} = -\frac{2}{3} g_s \mu_0 \frac{\mu_B}{\hbar}\,|\psi_{n,\ell}(0)|^2\,\mathbf{S} \tag{2.64}$$

This means that our perturbing Hamiltonian becomes

$$\boxed{\delta H_{HF} = A_J\,\mathbf{I}\cdot\mathbf{J}, \quad A_J = \frac{2}{3}\mu_0 \mu_N \mu_B g_s g_I \frac{|\psi_{n,\ell}(0)|^2}{\hbar^2}} \tag{2.65}$$

where we have written that $\mathbf{J} = \mathbf{S}$ as $L = 0$. It turns out that the form of this Hamiltonian is the same for electrons with non-zero values of angular momentum, which is why it has been stated as such here. We could have also argued this from the vector model; as the nuclear interaction is weak, only the precession around $\mathbf{J}$ is seen by the nucleus, and so $\mathbf{B}_e = (\text{scalar})\,\mathbf{J}$.

In the spin-orbit interaction, both $\mathbf{L}$ and $\mathbf{S}$ precessed around the total angular momentum $\mathbf{J}$, which remained a constant of the motion. By analogy, let us introduce the quantity

$$\mathbf{F} = \mathbf{I} + \mathbf{J}, \quad F = |I - J|, \dots, I + J \tag{2.66}$$

which is known as the *total atomic angular momentum*. This means that $\mathbf{F}^2$ and F_z are constants of motion, as well as $\mathbf{I}^2$ and $\mathbf{J}^2$. Thus, we adopt the eigenstates $|F, M_F, I, J\rangle$, allowing us to write the energy shift as

$$\delta E_{HF} = \frac{A_J}{2}\left(F(F+1) - I(I+1) - J(J+1)\right)\hbar^2 \tag{2.67}$$

The splitting will thus create either $2I + 1$ levels if $J > I$, or $2J + 1$ levels if $I > J$; this comes from the degeneracy associated with F.

A hyperfine transition occurs at 494 nm in single ionised ^{133}Cs *(cesium) between a level from the* $5p^5 6s$ *configuration, and one from the* $5p^5 6p$ *configuration. Five hyperfine structure components are observed with wavenumbers relative to that with the lowest wavenumber as follows:* 0.0, 8.1, 19.5, 33.7, 51.3 m^{-1}. *The experimental uncertainty in the position of each component is of order* 0.1 m^{-1}. *Find the nuclear spin of* ^{133}Cs*, and the value of* J *for the level arising from the* $5p^5 6s$ *configuration.*

As we are just given relative wavenumber separations, we need to derive a selection rule in order to tackle this problem. Consider the energy separation between adjacent levels:

$$\Delta E_{F,F-1} = \delta E_{HF}(F) - \delta E_{HF}(F-1) = \frac{A_J}{2}(F(F+1) - F(F-1)) = A_J F \tag{2.68}$$

Repeating this for another adjacent pair of energy levels, we can find the expression

$$\frac{\Delta E_{F,F-1}}{\Delta E_{F-1,F-2}} = \frac{F}{F-1} \equiv R \tag{2.69}$$

We can invert this expression for R as follows:

$$F = \frac{R}{R-1} \tag{2.70}$$

We can label the hyperfine levels relative to the maximum level ($F_{max} = 51.3\ \mathrm{m}^{-1}$). Using (2.70) for three pairs of levels, one can show that $F_{max} \backsim 11/2$ to within experimental uncertainty. From above, we know that

$$2(\text{smaller of } I/J) + 1 = \#\text{ of hyperfine levels} \tag{2.71}$$

so it follows that I or J is equal to 2. The last piece of information that we need comes from the configuration $5p^5 6s$; this has $S = 0, 1$, $L = 1$, and thus $J = 0, 1, 2$. This means that $J = 2$, allowing us to conclude that $I = 7/2$.

2.4 Magnetic Field Effects

We are now going to investigate the effect of applying a magnetic field to an atom that is described by the Hamiltonian (1.22). The Hamiltonian describing this interaction is given by

$$\boxed{\delta H_B = -\boldsymbol{\mu} \cdot \mathbf{B}_{\text{ext}}} \tag{2.72}$$

where $\boldsymbol{\mu}$ is now the magnetic moment of the entire atom at the structural level that we are considering. We take the magnetic field to be along the z-axis as a convenient choice of coordinate system. The splitting of spectral lines due to the application of such a field is known as the *Zeeman effect*.

2.4.1 Magnetic fields and Fine Structure

In this case, we define the strength of the magnetic field in comparison to the energy associated with the fine structure perturbation. That is, we have that

- Weak field: $\mu_B B_{\text{ext}} \ll \langle \delta H_{SO} \rangle$
- Strong field: $\mu_B B_{\text{ext}} \gg \langle \delta H_{SO} \rangle$

However, it is worth remembering that in almost all cases $\mu_B B \ll \langle \delta H_{RE} \rangle$; the magnetic field would have to be very large in order to compete with the residual electrostatic interaction.

Weak field limit

Let us initially consider the case where spin has been neglected, such that the magnetic dipole is given by (2.29) with $\mathbf{S} = 0$. This is known as the *Normal Zeeman effect*. In this case, we adopt the basis $|L, M_L\rangle$, allowing us to write the first order energy shift as

$$\delta E_B = \frac{\mu_B}{\hbar} B_{\text{ext}} \langle L, M_L| L_z |L, M_L\rangle = \mu_B M_L B_{\text{ext}} \tag{2.73}$$

The magnetic field thus splits a given energy level into $2L+1$, and the new levels are equally separated as M_L has to be integer. In spectral line transitions, we have the selection rule that $\Delta M_L = 0, \pm 1$ (see section 3.1.2), and so the spectral lines are split into three evenly space transitions with frequencies

$$\omega_0, \quad \omega_0 \pm \delta\omega, \quad \delta\omega = \frac{\mu_B B_{\text{ext}}}{\hbar} \tag{2.74}$$

We can now re-introduce the effect of spin. This is known as the *Anomalous Zeeman effect*, so-called because when it was first observed, spin had not been discovered, and the whole thing seemed a bit odd. In this case, the perturbation is given by

$$\boxed{\delta H_B = \frac{\mu_B}{\hbar}(\mathbf{L} + 2\mathbf{S}) \cdot \mathbf{B}} \tag{2.75}$$

where we have used (2.29) assuming that $g_s \backsim 2$. Then, it is clear that $\mathbf{J}^2$, J_z, $\mathbf{L}^2$, $\mathbf{S}^2$ all commute with the perturbation, meaning that we can adopt the eigenstates $|J, M_J, L, S\rangle$. The first order change in the energy is given by

$$\delta E_B = \frac{\mu_B}{\hbar} B_{\text{ext}} \langle J, M_J, L, S| (L_z + 2S_z) |J, M_J, L, S\rangle = \frac{\mu_B}{\hbar} B_{\text{ext}} (M_J \hbar + \langle S_z \rangle) \tag{2.76}$$

where we have used the fact that $J_z = L_z + S_z$. We can now employ a corollary of the Wigner-Eckart theorem, which states that:

$$\langle J, M_J| \mathbf{v} \left|J', M_J'\right\rangle \propto \langle J, M_J| \mathbf{J} \left|J', M_J'\right\rangle \tag{2.77}$$

That is, the expectation value of any vector operator $\mathbf{v}$ in a basis where total angular momentum is conserved (i.e. J and M_J are good quantum numbers) is proportional to the expectation value of $\mathbf{J}$ in that state. Thought of in terms of the vector model, this describes how any component perpendicular to $\mathbf{J}$ is time-averaged to zero due to procession around this axis. We thus write

$$\langle J, M_J, L, S|\, \mathbf{S}\, |J, M_J, L, S\rangle = \langle \mathbf{S}\rangle = c\,\langle \mathbf{J}\rangle \tag{2.78}$$

for some constant of proportionality c. Taking the dot product with $\mathbf{J}$:

$$\langle \mathbf{J}\cdot\mathbf{S}\rangle = cJ(J+J)\hbar^2 \quad\longrightarrow\quad c = \frac{\langle \mathbf{J}\cdot\mathbf{S}\rangle}{J(J+1)\hbar^2} \tag{2.79}$$

It follows that

$$\langle S_z\rangle = \frac{\langle \mathbf{J}\cdot\mathbf{S}\rangle\langle J_z\rangle}{J(J+1)\hbar^2} = \frac{M_J\,\langle \mathbf{J}\cdot\mathbf{S}\rangle}{J(J+1)\hbar^2} \tag{2.80}$$

We then note that

$$\mathbf{J}\cdot\mathbf{S} = \frac{1}{2}(\mathbf{J}^2 - \mathbf{L}^2 + \mathbf{S}^2) \tag{2.81}$$

such that the Anomalous Zeeman energy shift is given by

$$\boxed{\delta E_B = M_J\mu_B B_{\text{ext}}\left[1 + \frac{J(J+1) - L(L+1) + S(S+1)}{2J(J+1)}\right]} \tag{2.82}$$

It is clear from this equation the degenerate energy levels corresponding to a given J are split into $2J+1$ levels, proportionally to the applied magnetic field. This allows us to determine J for an atom, and thus other quantum numbers. The bracketed term is denoted g_J, and is known as the Landé g-factor. This constant of proportionality is usually positive, but can become negative when the projection of the total magnetic dipole moment onto $\mathbf{J}$ is positive (such as in the state $^6F_{1/2}$).

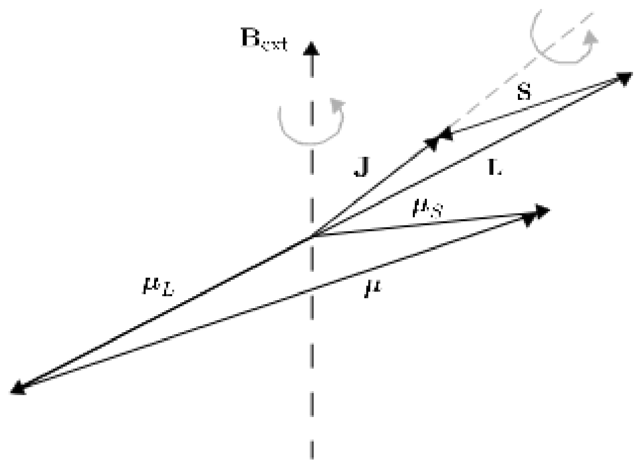

Figure 2.7: An example of how g_J can be negative according to the vector model. Note how the magnetic moments are in the opposite direction to their associated operators

Draw out the energy level diagram, together with the transitions, for the 671 nm transition in ^6Li ($Z = 3$), $1s^2s^2S_{1/2}$ - $1s^22p^2P_{3/2}$ in a weak field of magnitude B. Give the spacing of the frequency components.

As the Zeeman effect splits J into $2J+1$ levels, we are expecting 4 lines for the $1s^2 2p^2 P_{3/2}$ level ($g_J = 4/3$), and 2 lines for the $1s^2 2s^2 S_{1/2}$ level ($g_J = 2$). In all transitions, we require that $\Delta L = \pm 1$. The transitions where $\Delta M_J = \pm 1$ are known as 'σ' transitions, where as those with $\Delta M_J = 0$ are 'π' transitions. When observing along the magnetic field ($\mathbf{e}_z$), we see only σ transitions, where as we see both σ and π transitions when observing perpendicular to $\mathbf{B}$. See section 3.1.2 for more details concerning these selection rules.

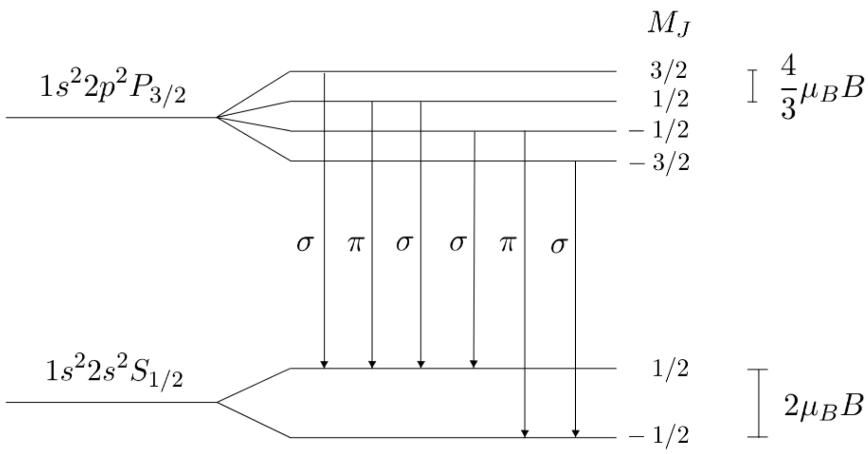

Figure 2.8: The Zeeman effect for a particular transition in Lithium (Li)

We can then calculate the relative frequency shift using *Professor Hooker's Energy Level Table* (patent pending):

		$^2P_{3/2}$ ($g_J = 4/3$)			
		-3/2	-1/2	1/2	3/2
$^2S_{1/2}$ ($g_J = 2$)	-1/2	-1	1/3	5/3	
	1/2		-5/3	-1/3	1

To compute the cell values, one takes the g_J corresponding to the top row of M_J values, multiplies it by M_J, and then subtracts a similar product for the left hand column. Cells that have been struck out correspond to transitions that are not allowed. This gives us the following transition relative frequency diagram:

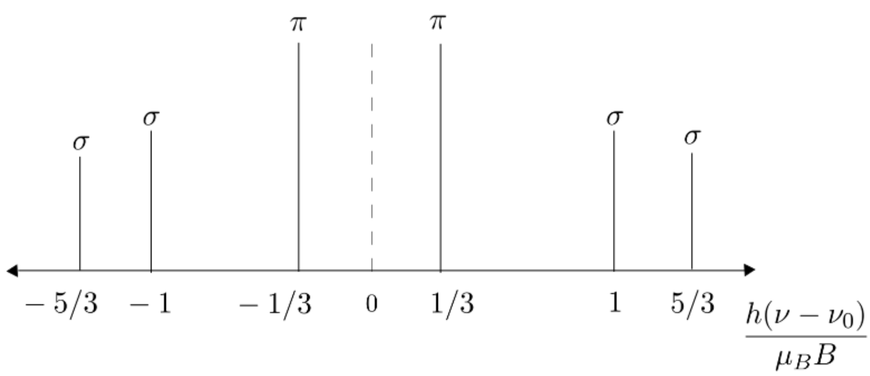

Figure 2.9: The relative frequency shifts due to the Zeeman effect for a particular transition in Lithium (Li). ν_0 is the central frequency given by $\nu_0 = \bar{\nu} c = 4.4 \times 10^5$ GHz.

Strong field limit

Under the strong field limit, the assumption that we can ignore the external torque that the magnetic field applies to the system breaks down. This means that $\mathbf{J}^2$ is no longer a constant of the motion, and so we use $\mathbf{L}^2$, L_z, $\mathbf{S}^2$, S_z to characterise the state of our system; this is because the strength of the external magnetic field has caused the orbital and spin angular momenta to de-couple, and so they individually precess around $\mathbf{B}_{\text{ext}}$. The resultant energy shift is given by

$$\delta E_B = \frac{\mu_B}{\hbar} B_{\text{ext}} \langle L, M_L, S, M_L| (L_z + 2S_z) |L, M_L, S, M_S\rangle = \mu_B (M_L + 2M_S) B_{\text{ext}} \quad (2.83)$$

It is usually very difficult to observe the Paschen-Back effect in practise, as it usually requires a very strong magnetic field. For example, for two energy levels separated by $\delta E = 0.01$ eV,

$$B_{\text{ext}} \backsim \frac{\delta E}{\mu_B} \backsim 173 \text{ T} \quad (2.84)$$

This sort of size of magnetic field is not readily achievable, given that the largest magnetic fields that have been created in laboratory environments are of order $\backsim 10$ T.

2.4.2 Magnetic fields and Hyperfine structure

In the case of hyperfine structure, we define the strength of the magnetic field in comparison to the energy associated with the fine structure perturbation. That is, we have that

- Weak Field: $\mu_B B_{\text{ext}} \ll A_J$
- Strong Field: $\mu_B B_{\text{ext}} \gg A_J$

where A_J is the coupling constant for hyperfine structure. The latter limit is usually readily achieved, as only a small magnetic field is required for it to dominate in comparison to the relatively small magnitude of the hyperfine structure energy.

Being in the hyperfine regime, we need to be wary of the fact that the nuclear spin can now contribute to the magnetic moment of the atom. Namely, we have that

$$\boldsymbol{\mu} = -g_J \frac{\mu_B}{\hbar} \mathbf{J} + g_I \frac{\mu_N}{\hbar} \mathbf{I} \quad (2.85)$$

However, we observe that $\mu_N \ll \mu_B$, meaning that we can actually neglect the contribution due to the second term, giving us

$$\boxed{\delta H_B = g_J \frac{\mu_B}{\hbar} \mathbf{J} \cdot \mathbf{B}_{\text{ext}}} \quad (2.86)$$

This is a curious result, as the above Hamiltonian does not explicitly depend on the nuclear spin. However, the resultant energy shift *does* depend on hyperfine structure due to the way in which we characterise our states in the strong and weak field limits.

Weak field limit

If the field is sufficiently weak, then we can assume that it applies no external torque on the system, meaning that $\mathbf{F}^2$ and F_z are constants of the motion. Thought of in terms of the vector model, this means that $\mathbf{J}$ and $\mathbf{I}$ precess about the resultant $\mathbf{F}$, which itself precesses around $\mathbf{B}_{\text{ext}}$. This means that we consider the projection of $\mathbf{J}$ onto $\mathbf{F}$:

$$\delta H_B = g_J \frac{\mu_B}{\hbar} \frac{\langle \mathbf{J} \cdot \mathbf{F}\rangle}{F(F+1)\hbar^2} \mathbf{F} \cdot \mathbf{B}_{\text{ext}} \quad (2.87)$$

Once again aligning $\mathbf{B}_{\text{ext}}$ along the z-axis, and observing that

$$\mathbf{J} \cdot \mathbf{F} = \frac{1}{2}(\mathbf{F}^2 - \mathbf{I}^2 + \mathbf{J}^2) \tag{2.88}$$

it becomes clear that the energy shift can be written as

$$\boxed{\delta E_B = g_F M_F \mu_B B_{\text{ext}}, \quad g_F = \frac{F(F+1) - I(I+1) + J(J+1)}{2F(F+1)} g_J} \tag{2.89}$$

Analogously to the Zeeman effect for fine structure, we see that the magnetic field splits the degenerate energy levels into $2F+1$ separate magnetic energy levels, proportionally to the applied field. We see from the above expression for g_F that the nuclear spin makes a contribution to the energy shift; this is because $\mathbf{I}$ itself is not small, even though the nuclear magnetic moment is.

Strong field limit

In a similar vein to the Paschen-Back effect, we argue that in the strong field limit, $\mathbf{J}$ and $\mathbf{I}$ decouple and individually precess around $\mathbf{B}_{\text{ext}}$. In this case, we write the Hamiltonian as

$$\delta H_B = g_J \mu_B \mathbf{J} \cdot \mathbf{B}_{\text{ext}} + A_J \mathbf{I} \cdot \mathbf{J} \tag{2.90}$$

where we have included the δH_{HF} term (2.65) to make the energy separation between the resultant levels more explicit. We adopt the eigenstates $|J, M_J, I, M_I\rangle$, meaning that the energy shift is given by

$$\delta E_B = g_J M_J \mu_B B_{\text{ext}} + \langle J, M_J, I, M_I | A_J \mathbf{I} \cdot \mathbf{J} | J, M_J, I, M_I \rangle \tag{2.91}$$

The second of these terms can be evaluated explicitly using the ladder operators

$$I_\pm = I_x \pm i I_y, \;\; J_\pm = J_x \pm i J_y \tag{2.92}$$

It can be shown that these operators act according to

$$I_\pm |J, M_J, I, M_I\rangle \propto |J, M_J, I, M_I \pm 1\rangle, \;\; J_\pm |J, M_J, I, M_I\rangle \propto |J, M_J \pm 1, I, M_I\rangle \tag{2.93}$$

Then:

$$\mathbf{I} \cdot \mathbf{J} = I_x J_x + I_y J_y + I_z J_z = \frac{1}{2}(I_+ J_- + I_- J_+) + I_z J_z \tag{2.94}$$

It is clear from the above expression that all but the components along the magnetic field ($\mathbf{e}_z$) will have zero expectation value in this basis. Putting this together, the energy level shift is then given by

$$\boxed{\delta E_B = g_J M_J \mu_B B_{\text{ext}} + A_J M_I M_J} \tag{2.95}$$

The first term describes the precession of $\mathbf{J}$ around $\mathbf{B}_{\text{ext}}$, while the second describes the corresponding precession of the nuclear spin $\mathbf{I}$. The strong field states are split into states labelled by M_J, each of which are split into $2I+1$ sub-levels according to the degeneracy in M_I. The separation of the sub-levels remains constant as you increase $\mathbf{B}_{\text{ext}}$, while the separation of the M_J levels increases proportionally.

Consider the following diagram of hyperfine Zeeman splitting, labelled with the appropriate quantum numbers. Deduce the nuclear spin of the isotope, and the sign of g_F. The measured zero field splitting is 327.4 MHz. Find the separation of adjacent states in the strong field limit.

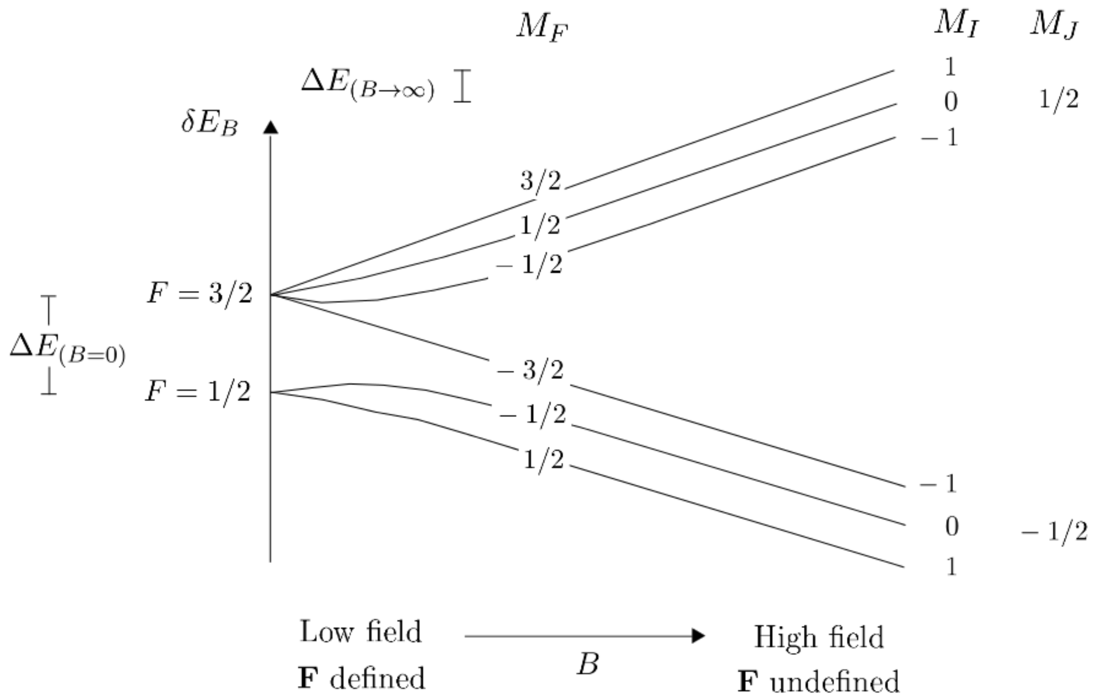

Figure 2.10: The Zeeman effect in hyperfine splitting

Before calculating g_F, it will be useful to examine how the quantum numbers shown on the diagram were assigned. Let us initially consider the high field limit. We know that the large energy splitting becomes dominated by the normal Zeeman effect, which creates $2J+1$ levels, indexed by M_J. It is clear from the diagram that we have two 'sets' of hyperfine levels, allowing us to conclude that $J=1/2$, and consequently M_J from the fact that $-J<M_J<J$. The second term in (2.95) splits each of the levels in M_J into $2I+1$ sub-levels, allowing us to then conclude that $I=1$. We then consider the low field limit. The application of the magnetic field splits each F level into $2F+1$ sub-levels, which gives us the labels at the left hand side of the diagram. We then use the fact that $M_F=M_I+M_J$ is a good quantum number in both the high field and low field limits to deduce M_F. It trivially follows that $g_J=0$, implying that $g_F=-2/3$ for $F=1/2$, $g_F=2/3$ for $F=3/2$.

The zero field splitting is given by (2.67), meaning that we can write the energy difference $\Delta E_{(B=0)}$ as

$$\Delta E_{(B=0)} = \frac{A_J}{2}\left(\frac{3}{2}\left(\frac{5}{2}\right)-\frac{1}{2}\left(\frac{3}{2}\right)\right)\hbar^2 = \frac{3}{2}A_J\hbar^2 \tag{2.96}$$

In the high field limit, the separation $\Delta E_{(B\to\infty)}$ is due to the second term in (2.95). In both cases, $|M_J|=1/2$, and so

$$\Delta E_{(B\to\infty)} = \frac{1}{2}A_J\hbar^2 = \frac{1}{3}\Delta E_{(B=0)} = 0.45\times10^{-6}\ \text{eV} \tag{2.97}$$

3. *Radiation*

In this chapter, we will examine the theory behind transitions and radiation within atoms, including

- Radiative Transitions
- Inner Shell Transitions
- Thermal Radiation

The previous two chapters was focussed mainly on outlining the various energy levels that are present in the atom, given the perturbative level being considered. We are now going to look at what happens when there are radiative transitions between these levels. This is an important aspect to round off our examination of the atom, as it is usually through observing these transitions that we can make deductions about atomic structure.

3.1 Radiative Transitions

As stated at the start of this chapter, radiative transitions occur between atomic energy levels in atoms, usually induced as a result of external excitation, such as an incoming electromagnetic wave. We can model the effects of such excitation as a time-dependent perturbation on our system such that $H = H_0 + \delta H(t)$, where $H_0 = H_{\text{atomic}}$ as given by (1.22). We then propose that we can write the resultant state of the system as

$$|\psi, t\rangle = \sum_n a_n(t)\, e^{-iE_n t\hbar} |n\rangle \tag{3.1}$$

This expression includes the implicit assumption that the energy eigenvalues E_n and eigenstates $|n\rangle$ are fixed by H_0, and only the coefficients that determine the superposition of states change with time. We can then substitute this into the TDSE: Substitute this into the TDSE:

$$\sum_n e^{-iE_n t/\hbar} (i\hbar \dot{a}_n + \cancel{E_n a_n}) |n\rangle = \sum_n e^{-iE_n t/\hbar} a_n (\cancel{H_0 |n\rangle} + \delta H |n\rangle) \tag{3.2}$$

$$i\hbar \sum_n \dot{a}_n e^{-iE_n t/\hbar} |n\rangle = \sum_n e^{-iE_n t/\hbar} a_n \delta H |n\rangle \tag{3.3}$$

Bra through by $\langle m|$ and $\frac{1}{i\hbar} e^{iE_m t/\hbar}$:

$$\boxed{\dot{a}_m = -\frac{i}{\hbar} \sum_n e^{i(E_m - E_n)t/\hbar} \langle m| \delta H |n\rangle a_n} \tag{3.4}$$

The above expression is a set of coupled differential equations for the time evolution of the coefficients of the system. Let us now consider a the case of a sinusoidal perturbation on the system of the form:

$$\delta H(t) = V_0 e^{\mp i\omega t} \tag{3.5}$$

Let $\omega_{nm} = (E_m - E_n)\hbar$, meaning that our amplitude for the transition can be written as

$$a_m = -\frac{i}{\hbar} \int dt\, e^{i\omega_{nm} t} \langle m| \delta H |n\rangle = -\frac{1}{\hbar} \langle m| V_0 |n\rangle \frac{e^{i(\omega_{nm} \mp \omega)t} - 1}{\omega_{nm} \mp \omega} \tag{3.6}$$

assuming that $a_n = \delta_{nm}$. In other words, we have assumed that the system was initially in state n upon the application of the perturbation. This has associated probability

$$P_{nm} = \frac{|\langle m| V_0 |n\rangle|^2}{\hbar^2} \frac{\sin^2\left(\frac{\omega_{nm} \mp \omega}{2} t\right)}{\left(\frac{\omega_{nm} \mp \omega}{2}\right)^2} \tag{3.7}$$

3.1.1 Electric Dipole Approximation

Now we consider the case of an incoming electromagnetic wave. As $\lambda \gg a_0$ for most incident radiation, we can consider the strength of both the electric and magnetic fields to be constant over the transition cross section σ. Furthermore, as the force due to the magnetic field is significantly less than that due to the electric field, we can neglect it's contribution. This is known as the *electric dipole approximation.* We can represent a uniform oscillating field of strength E_0

$$\delta H(t) = e|\mathbf{p}|\, e^{-i\omega t}, \quad p = E_0 \mathbf{x} \tag{3.8}$$

If we are considering a transition between two discrete energy level E_n and E_m (as is the case in atomic structure), then ω_{nm} remains fixed. However, there may be a range of frequencies in the incoming radiation with which we associate a spectral energy density $\rho(\omega)$, defined by:

$$\int_0^\infty d\omega\ \rho(\omega) = \frac{1}{2}\epsilon_0 E_0^2 \tag{3.9}$$

Noting that in this case $V_0 = eE_0|\mathbf{x}|$, it becomes clear that we can write the transition probability as

$$P_{nm} = \frac{2e^2}{\epsilon_0\hbar^2}|\langle m|\,\mathbf{x}\,|n\rangle|^2 \int_0^\infty d\omega\ \rho(\omega)\frac{\sin^2\left(\frac{\omega_{nm}-\omega}{2}t\right)}{\left(\frac{\omega_{nm}-\omega}{2}\right)^2} \tag{3.10}$$

The integrand of the above expression is dominated by a sharp peak around $\omega = \omega_{nm}$, and so we can argue that we can approximate the spectral energy density as being constant over the region of integration. This allows us to write

$$\int_0^\infty d\omega\ \rho(\omega)\frac{\sin^2\left(\frac{\omega_{nm}-\omega}{2}t\right)}{\left(\frac{\omega_{nm}-\omega}{2}\right)^2} \backsim \rho(\omega_{nm})2t\int_0^\infty dx\ \frac{\sin^2 x}{x^2} = \pi t\rho(\omega_{nm}) \tag{3.11}$$

We can thus finally write our transition rate as

$$\boxed{R_{mn} = \frac{2\pi e^2}{3\epsilon_0\hbar^2}|\langle n|\,z\,|n\rangle|^2\rho(\omega_0)} \tag{3.12}$$

The factor of three in the denominator comes from the fact that we have to average $\mathbf{x}$ over all of the possible spatial orientations of the atom (isotropic system).

3.1.2 Selection rules

Taking our eigenstates to be those of the gross atomic structure $|n,\ell,m_\ell\rangle$, it is clear that the transition rates are proportional to $\langle n',\ell',m_\ell'|\,\mathbf{v}\,|n,\ell,m_\ell\rangle$ in the electric dipole approximation. If any of these matrix elements are zero, then the transition is forbidden, leading to what are known as *selection rules*. These are as follows:

- The emitted photon for the transition carries off one unit of angular momentum, so $|J-J'| = 1$ is possible. It is also possible to have $|J-J'| = 0$; this occurs where the spin and orbital angular momentum of the atom reconfigure themselves (after the release of the photon) such that $|J-J'| = 0$. This follows from the fact that $J = |L_S|\dots L+S$, meaning that the same value of J may be still be present after the transition. Evidently, this cannot occur for $J=0$.

- The dipole operator $\mathbf{v} = e\mathbf{p}$ has no effect on the spin of the wavefunction, and so the spin cannot change, implying $M_S = M_S'$. This is only the case if we do not account for LS coupling effects.

- Let us consider the parity of the spherical harmonics. Suppose that

$$Y_\ell^\ell(\theta,\phi) = \langle\theta,\phi|\ell,\ell\rangle \tag{3.13}$$

for a single electron system. We then apply the raising operator $L_+ = L_x + iL_y$ to this state. Nothing that m_ℓ is at it's maximum value, it follows that

$$e^{i\phi}\left(\frac{\partial}{\partial\theta} + i\cot\theta\frac{\partial}{\partial\phi}\right)Y_\ell^\ell = 0 \tag{3.14}$$

Suppose that Y_ℓ^ℓ is an eigenstate of L_z such that $L_z Y_\ell^\ell = \ell\hbar Y_\ell^{\ell_i}$. This implies that $Y_\ell^\ell = f(\theta)e^{i\ell\phi}$ for some function f. Then:

$$\frac{\partial f}{\partial\theta} - \ell\cot\theta f(\theta) = 0 \longrightarrow \frac{\partial}{\partial\theta}\left(f(\theta)\sin^{-\ell}\theta\right) = 0 \tag{3.15}$$

We thus arrive at the important result of

$$\boxed{Y_\ell^\ell(\theta,\phi) \propto \sin^\ell\theta e^{i\ell\phi}} \tag{3.16}$$

In spherical polar coordinates, an application of the parity operator $\mathcal{P}$ gives rise to the transformation $[\theta,\phi] \mapsto [\pi-\theta,\phi+\pi]$. Applying this to (3.13):

$$\mathcal{P}\sin^\ell\theta e^{i\ell\phi} = \sin^\ell(\pi-\theta)e^{i\ell(\phi+\pi)} = (-1)^\ell \sin^\ell\theta e^{i\ell\phi} = (-1)^\ell \langle\theta,\phi|\ell,\ell\rangle \tag{3.17}$$

As the lowering and raising operator $L_- = L_x - iL_y$ is parity symmetric, applying it to the above state will not change its parity. This means that the parity of a general state is given by

$$\boxed{\mathcal{P}\,|n,\ell,m_\ell\rangle = (-1)^\ell\,|n,\ell,m_\ell\rangle} \tag{3.18}$$

The above result is true for a general state with good quantum numbers n, ℓ and m_ℓ. Now, we know that the expectation value of any vector operator is zero in a state of well-defined parity. This means that if both ℓ and ℓ' are odd or even, then both states are of the same parity, and the matrix element vanishes. This forces us to conclude that $|\ell-\ell'| = 1$. However, in the case of a multiple electron atom, the total orbital angular momentum may reconfigure itself, such that $|L-L'| = 0$. As above, this cannot occur for $L = 0 \to L' = 0$.

- Let us initially consider the case where radiation is incident along $\mathbf{z}$, meaning that $\mathbf{v} = e\mathcal{E}\mathbf{z}$. As $[L_z, z] = 0$, we can write that

$$L_z(z\,|n,\ell,m_\ell\rangle) = zL_z\,|n,\ell,m_\ell\rangle = m_\ell\hbar(z\,|n,\ell,m_\ell\rangle) \tag{3.19}$$

This means that $z\,|n,\ell,m_\ell\rangle$ is an eigenstate of L_z, and this orthogonal to all other eigenstates of L_z, leading us to conclude that $|m_\ell - m_\ell'| = 0$ along $\mathbf{z}$. Next, define the operators $x_\pm = x \pm iy$. It follows quickly from the commutation relation for angular momentum $[v_i, L_j] = i\hbar\epsilon_{ijk}v_k$ that $[L_z, x_\pm] = \pm\hbar x_\pm$. Then:

$$L_z(x_\pm\,|n,\ell,m_\ell\rangle) = x_\pm(L_z \pm 1)\,|n,\ell,m_\ell\rangle = (m_\ell \pm 1)(x_\pm\,|n,\ell,m_\ell\rangle)$$

So $x_\pm\,|n,\ell,m_\ell\rangle$ is an eigenket of L_z with eigenvalue $m_\ell \pm 1$. Given that x and y can both be written in terms of $x_\pm$, we conclude that the matrix elements for x and y are zero unless

$$|m_\ell - m_\ell'| = 1$$

for orthogonality reasons. This is easily generalised to multiple electrons.

In all these cases, n is allowed to change by an amount, but only one electron is able to make a transition at any given time. A useful summary of these results is included in the box below:

$$|J-J'| \leq 1 \quad \text{except for } J = 0 \to J' = 0 \tag{3.20}$$
$$|L-L'| \leq 1 \quad \text{except for } L = 0 \to L' = 0 \tag{3.21}$$
$$|M_J - M_J'| \leq 1 \quad \text{except } M_J = 0 \to M_J' = 0 \text{ if } |J-J'| = 0 \tag{3.22}$$
$$|M_L - M_L'| = 0 \quad \text{for } z \tag{3.23}$$
$$|M_L - M_L'| = 1 \quad \text{for } x, y \tag{3.24}$$
$$|M_S - M_S'| = 0 \tag{3.25}$$

Once again, we draw the readers attention to the fact that the above quantum numbers are the composite eigenvalues. In the case of a single particle, both j and ℓ must change by one.

3.2 Inner Shell Transitions

Thus far, we have only been concerned with the energy levels of the valence electrons (those that are outside filled electron shells). As stated previously, transitions between such energy levels typically are of order $\backsim 10$ eV to $\backsim 10^{-6}$ eV, as the energy differences involved are typically quite small. Transitions between inner electron shells are much more energetic (typically of order keV), meaning that the emitted radiation is in the form of x-rays. X-ray transitions occur between the inner electron shells of atoms when high energy photons or electrons bombarding the atom create an inner shell vacancy. This allows an electron to transition from a higher energy level to a lower one by the emission of an X-ray photon.

3.2.1 Characteristic X-Rays

For the inner shell electrons, the central field of the nucleus is approximately of the from of a Coulomb field, and so we approximate the energy levels as being hydrogenic, of the form:

$$\boxed{E_n = -\frac{1}{2}\mu(\alpha c)^2\frac{(Z-\sigma_n)^2}{n^2}} \tag{3.26}$$

In a similar way to with alkali elements, we take account of the fact that the system is not purely hydrogenic through defining an effective nuclear charge $Z_{eff} = Z - \sigma_n$. The parameter σ_n is a *screening factor* that take into account the amount by which the electrons within the two energy levels experience screening of the nucleus due to other electrons that are not involved in the transition. The value of this screening factor depends quite obviously on the electrons inside the given energy level that we are considering, but it also depends on the outer electrons, as these define the potential of the given level *relative to infinity.* Typically, these screening factors are factors of order unity, and are determined empirically.

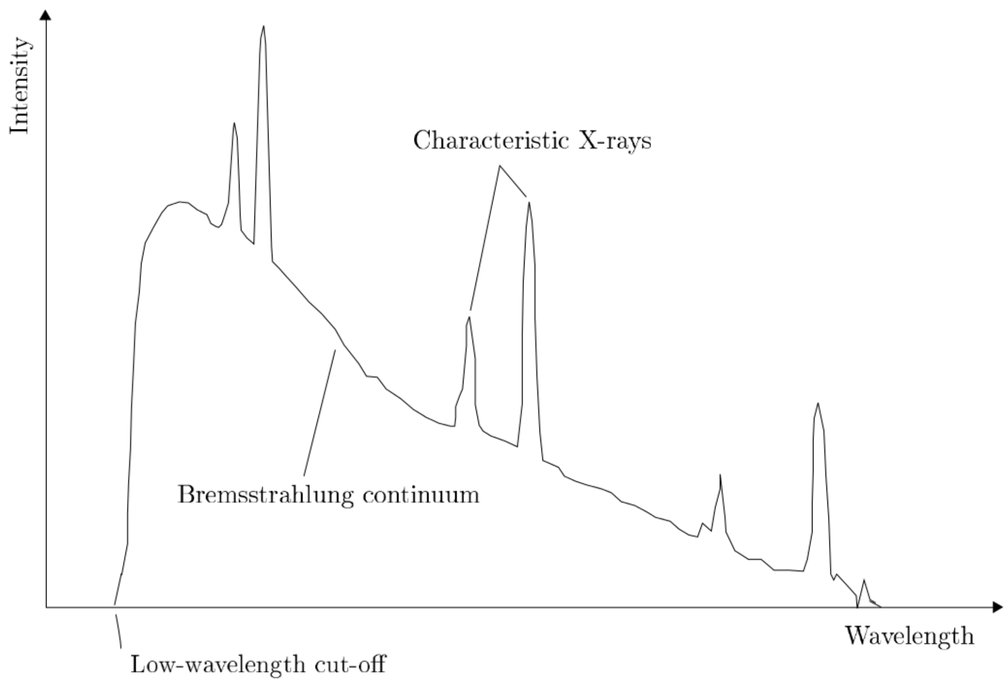

Figure 3.1: An X-ray spectrum for Lithium Flouride Crystal (LiF), showing the Bremsstrahlung continuum, and characteristic X-ray peaks

The energies of the X-ray transitions are then given by the difference in energy between these two levels. For a transition $n \mapsto m$, this is given by:

$$\Delta E_{nm} = \frac{1}{2}\mu(\alpha c)^2 \left(\frac{(Z-\sigma_n)^2}{n^2} - \frac{(Z-\sigma_m)^2}{m^2} \right) \tag{3.27}$$

We can observe these transitions using (for example) X-ray spectroscopy, involving bombarding an sample of a particular element with high-energy electrons emitted from an X-ray tube. This creates a continuous spectrum due to the *Bremsstrahlung* or *breaking* radiation due to the deceleration of the tube electrons as they interact with the atomic nuclei. There is a low-wavelength cut-off that occurs where all the energy of the electron is emitted as breaking radiation, bringing an end to the continuum. This means that the Bremsstrahlung continuum is actually characteristic of the tube voltage, rather than the specific element under study.

Superimposed on this continuum we have the characteristic X-rays emissions that correspond to inner shell transitions, with energies given by (3.27). These usually come in various groups that correspond to transitions to $n = 1, 2, 3, \ldots$, known as the K-series, L-series and M-series. One usually only observes three such series due to the fact that transitions to $n = 4$ are often not energetic enough to create X-rays upon emission. Note that the term *primary electrons* is sometimes used to refer to the electrons that are ionised due to incoming radiation. The difference between their kinetic energy and the energy of the incoming radiation gives the binding energies of the various energy levels. Pay attention to selection rules when finding the characteristic X-rays; some transitions are not allowed!

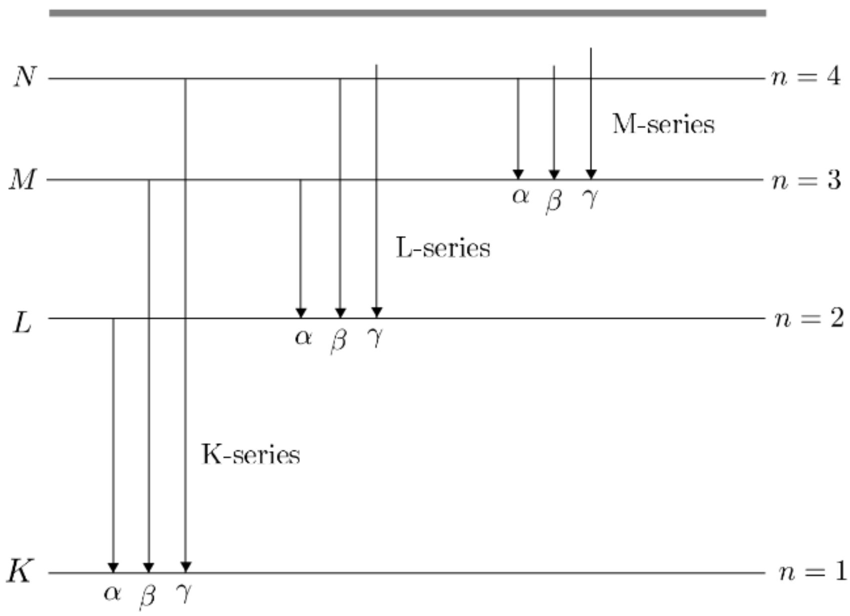

Figure 3.2: An energy level diagram showing the various X-ray series, as well as the individual lines (e.g. $K_\alpha, K_\beta, \ldots$)

A X-ray tube operates with a tungsten target ($Z = 74$). As the tube voltage is increased, three groups of lines appear. The first appears at a tube voltage of $\backsim$ 2.5 kV, with wavelengths around 0.65 nm. The second appears at $\backsim$ 12 kV, the wavelengths being around 0.13 nm. Estimate the tube voltage at which the final group appears, and the wavelength of *the strongest line in the group.*

As the mass of the tungsten nucleus is very large, we can assume that $\mu \backsim m_e$, meaning that the energy of the lowest K level is given by

$$E_K = \frac{1}{2}m_e(\alpha c)^2(Z-\sigma_K)^2 = hcR_\infty(Z-\sigma_K)^2 \tag{3.28}$$

For $Z \gg 1$, it is safe to estimate σ_K as some small integer such that $\sigma_K \ll Z$. This means that the threshold voltage for the K series can be calculated as

$$V_K \backsim \frac{E_K}{e} \backsim 67 \text{ kV} \tag{3.29}$$

The energy of the longest wavelength in the group is then given by the difference in energy between the $n = 1$ and $n = 2$ levels (see figure 3.2), which we can deduce from the tube voltages.

$$\Delta E_{21} = q(V_K - V_L) \quad \longrightarrow \quad \lambda \backsim 20 \text{ pm} \tag{3.30}$$

3.2.2 X-ray fine structure

A single vacancy in an otherwise full shell has the properties of a single electron in an otherwise empty shell (this arises from symmetry arguments). This means that our assumption that the X-ray energy levels are hydrogenic is valid. As such, these energy levels are split by the spin-orbit interaction to give fine structure components, separated by

$$\Delta E_{FS} = \frac{\mu_0\mu_B^2}{2\pi}\frac{Z^4}{(na_0)^3}\frac{1}{\ell(\ell+1)} \tag{3.31}$$

This expression can be derived by considering the difference in energy between two fine structure levels for a hydrogenic atom, such that $j = \ell \pm s$ and $s = 1/2$. This gives rise to a multiplet structure of X-ray lines (usually doublets and triplets), subject to the selection rules outlined in section 3.1.2. For example, the K_α doublet (denoted $K_{\alpha 1}$ and $K_{\alpha 2}$) exists because this is transition from a $2p$ level that has two possible values of j.

3.2.3 The Auger effect

The Auger effect occurs where an electron undergoing an X-ray transition imparts its energy to another electron (not necessarily in the same energy level), instead of releasing a photon. If the energy is sufficient, this second electron is ionised. The resultant kinetic energy of the electron will be

$$\boxed{T = E_{\text{trans}} - E_{\text{bind}}} \tag{3.32}$$

where E_{trans} is the energy corresponding to the transition of the initial electron, and E_{bind} is the binding energy associated with the electron to which the energy is imparted. Evidently, if T comes out to be negative, the Auger transition does not occur. As this effect is not under the electric dipole approximation, Auger transitions do not have to obey selection rules.

There will now be two inner shell vacancies, which will either be filled by X-ray transitions from higher energy states, or further Auger processes. As such, this process is doubly ionising. This dominates over radiative transitions for the elements of lower Z, meaning that more doubly-ionised atoms will be present than singly ionised atoms upon the analysis of such elements. A further subtle point to note is that when the initial vacancy is created, the atom is no longer neutral. This will actually increase the binding energy that the Auger electron has to overcome, meaning that our value for T above might, in reality, be lower.

3.3 Thermal Radiation

In this section, we shall take some time to introduce some ideas and definitions that we will make use of in the next chapter. These mainly pertain to radiation from macroscopic bodies, rather than from individual atomic systems, as we have thus far been concerned with.

3.3.1 Specific Intensity

We define the *specific intensity* I_ω of a radiating body as the energy emitted in the frequency range $[\omega, \omega + d\omega]$ per unit area, per unit time, per solid angle. This can be expressed as

$$dE = \frac{I_\omega}{2\pi}\, dSdtd\Omega d\omega \tag{3.33}$$

where $dS = \cos\theta dA$ is the differential surface area element. The total intensity is then obtained by integrating over the frequency range $[0, \infty]$.

In free space, where there is no absorption or emission of radiation, the specific intensity is preserved as the radiation propagates. Consider two surface elements dS_1 and dS_2 separated by some line element $d\ell$ along the direction of propagation of the radiation. Then, the energy passing through each is given by

$$dE_1 = \frac{I_{\omega 1}}{2\pi}\, dS_1dtd\Omega_1 d\omega \quad \text{and} \quad dE_2 = \frac{I_{\omega 2}}{2\pi}\, dS_2dtd\Omega_2 d\omega \tag{3.34}$$

However, by energy conservation, we require that $dE_1 = dE_2$. Noting that $dS_1 = d\ell d\Omega_1$ and $dS_2 = d\ell d\Omega_2$, it then follows that $I_{\omega 1} = I_{\omega 2}$. This can be expressed in differential form as

$$\boxed{\frac{dI_\omega}{d\ell} = 0} \tag{3.35}$$

This is essentially a statement of energy conservation. Let us also define a few integral moments of this quantity:

- Mean intensity - This is the average of I_ω over the solid angle:

$$J_\omega = \frac{1}{4\pi}\int d\Omega\, I_\omega \tag{3.36}$$

  This is particularly of use when evaluating the rates of physical processes that are photon dominated, but are independent of the angular distribution of the radiation, such as in photoexcitation and photoionisation.

- Radiation flux - This is the net rate of energy flowing across a unit area, per unit time, in the frequency range $[\omega, \omega + d\omega]$. As such, it is given by the first angular moment of I_ω.

$$P_\omega = \int d\Omega\, \cos\theta\, I_\omega \tag{3.37}$$

  The crucial difference to note between specific intensity and the flux is that while specific intensity is independent of the distance from the source, the flux obeys the inverse square law.

- Radiation pressure - This is the momentum flux; that is, the momentum delivered per unit time, per unit area, in the frequency range $[\omega, \omega + d\omega]$. It is related to the second angular moment of the distribution of I_ω as follows:

$$p_\omega = \frac{1}{c}\int d\Omega\, \cos^2\theta\, I_\omega \tag{3.38}$$

The extra factor of $\cos\theta$ comes from the fact that the radiation may be incident at some angle θ to the normal. Inside a reflecting enclosure, such as a blackbody (see section 3.3.2), this pressure is doubled as the photons are perfectly reflected, rather than being partially absorbed.

Find an expression for the radiation flux at a radial distance r from a sphere of radius R and uniform brightness.

Uniform brightness implies that the specific intensity is constant over the surface of the sphere: $I_\omega = B =$ constant. Define the angle

$$\theta_r = \sin^{-1}\left(\frac{R}{r}\right) \tag{3.39}$$

Then, the resultant flux is clearly given by

$$P_\omega = \int d\Omega\, \cos\theta I_\omega = B\int_0^{2\pi} d\phi \int_0^{\theta_r} d\theta\, \cos\theta\sin\theta = \pi B(1-\cos^2\theta_r) \backsim \pi\left(\frac{R}{r}\right)^2 \tag{3.40}$$

assuming that that $R \ll r$. We have thus confirmed that the radiation flux falls off as an inverse square law, as anticipated above.

3.3.2 Blackbody Radiation

An object that absorbs all radiation incident upon it is known as a *blackbody*. When it is at a uniform temperature, its emission has a spectral energy density profile that is only dependent on temperature, which is the defining characteristic of *blackbody radiation*.

We can model a blackbody as a cavity containing a gas of photons with energy per particle $\hbar\omega$. It follows that for a gas of N particles that the energy density is given by

$$u = u(T) = n\hbar\omega \tag{3.41}$$

From the kinetic theory of gases, we know that the particle flux is $\Phi = \frac{1}{4}nc$, meaning that the total energy flux is given by $P = \frac{1}{4}uc$. Lastly, we know that $p = \frac{2}{3}u$ for a general kinetic gas, and so we can write the pressure of the photon gas as $p = \frac{1}{3}u$. Using these equations, we can derive some further properties of blackbody radiation.

Stefan-Boltzmann Law

Recalling the equation for the internal energy U of the gas, it follows that

$$dU = TdS - \frac{u}{3}dV \quad\longrightarrow\quad \left(\frac{\partial U}{\partial V}\right)_T = T\left(\frac{\partial S}{\partial V}\right)_T - \frac{u}{3} \tag{3.42}$$

However, we know that

$$\left(\frac{\partial U}{\partial V}\right)_T = \frac{\partial}{\partial V}(uV)_T = u + V\left(\frac{\partial u}{\partial V}\right)_T = u \tag{3.43}$$

as u cannot depend on the size of the system by the definition. Recalling that the Helmholtz free energy is given by $F = U - TS$, we can use the following Maxwell relation

$$\left(\frac{\partial S}{\partial V}\right)_T = \left(\frac{\partial p}{\partial T}\right)_V = \frac{1}{3}\frac{du}{dT} \tag{3.44}$$

We thus obtain the differential equation

$$u = \frac{1}{3}T\frac{du}{dT} - \frac{u}{3} \longrightarrow 4u = T\frac{du}{dT} \tag{3.45}$$

that we can solve to obtain $u \propto T^4$. This means that *incident power per unit area* is given by

$$\boxed{P = \frac{1}{4}uc = \sigma T^4} \tag{3.46}$$

for some constant of proportionality σ that is known as the *Stefan-Boltzmann constant*. However, in order to find an exact expression for σ, we need to investigate how our energy is distributed in frequency space.

Plank distribution

The *spectral energy density* $\rho(\omega)$ is the energy density per unit volume, in the frequency range $[\omega, \omega + d\omega]$. The photons in our gas have two possible polarisation states ($s = \pm 1$), meaning that the density of states for such a system is given by

$$g(k)d^3\mathbf{k} = \underbrace{2}_{\text{polarisation states}} \frac{V}{(2\pi)^3}4\pi k^2 dk = \frac{Vk^2}{\pi^2}dk \tag{3.47}$$

Using the dispersion relation $\omega = ck$, this can be written as

$$g(\omega)d\omega = \frac{V}{\pi^2 c^3}\omega^2 d\omega \tag{3.48}$$

Assuming that the number of photons is large enough to approximate them as having a continuous spectrum, we can adopt Bose-Einstein statistics to write the mean occupation number for a particular state with energy $\hbar\omega$ as

$$\bar{n}_i = \frac{1}{e^{\beta\hbar\omega} - 1} \tag{3.49}$$

where we have defined $\beta \equiv k_B T$. The spectral energy density is thus given by

$$\boxed{\rho(\omega) = \bar{n}_i g(\omega)\hbar\omega = \frac{\hbar}{\pi^2 c^3}\frac{\omega^3}{e^{\beta\hbar\omega} - 1}} \tag{3.50}$$

This is known as the *Plank distribution*. We can then use this to find an expression for the Stefan-Boltzmann constant:

$$u = \int d\omega\, \rho(\omega) = \frac{\hbar}{\pi^2 c^3}\int_0^\infty d\omega\, \frac{\omega^3}{e^{\beta\hbar\omega} - 1} = \frac{\hbar}{\pi^2 c^3}\frac{1}{(\hbar\beta)^4}\underbrace{\int_0^\infty dx\, \frac{x^3}{e^x - 1}}_{\pi^4/15} \tag{3.51}$$

where we have made the substitution that $x = \beta\hbar\omega$. By comparison with (3.41), it is clear that the Stefan-Boltzmann constant can be expressed as

$$\boxed{\sigma = \frac{\pi^2 k_B^4}{60\hbar^3 c^2} = 5.67 \times 10^{-8}\ \mathrm{W\,m^{-2}K^{-4}}} \tag{3.52}$$

By letting $\omega = 2\pi c/\lambda$, we can also write the spectral energy density in wavelength space as

$$\rho(\lambda) = \frac{8\pi hc}{\lambda^5}\frac{1}{e^{\beta hc/\lambda} - 1} \tag{3.53}$$

When plotted, this gives the typical blackbody curves, as shown in In the classical limit, β becomes very small, so we can Taylor expand, yielding the *Rayleigh-Jeans law*:

$$\rho(\lambda) = \frac{8\pi k_B T}{\lambda^4} \tag{3.54}$$

This evidently diverges for low λ, giving infinite energy density, which is known as the *ultraviolet catastrophe*. We thus need the quantisation that is implicitly included in (3.53). This distribution has a maximum that can be found numerically as $\lambda_{\text{max}} \backsim (hc)/(5k_B T)$. This gives rise to *Wien's Law* which states that

$$\boxed{\lambda_{\text{max}} T = \text{constant}} \tag{3.55}$$

That is, the product of the maximum wavelength emitted by a black-body and it's temperature will yield a constant value. This can be used to find the temperature of stars, for example.

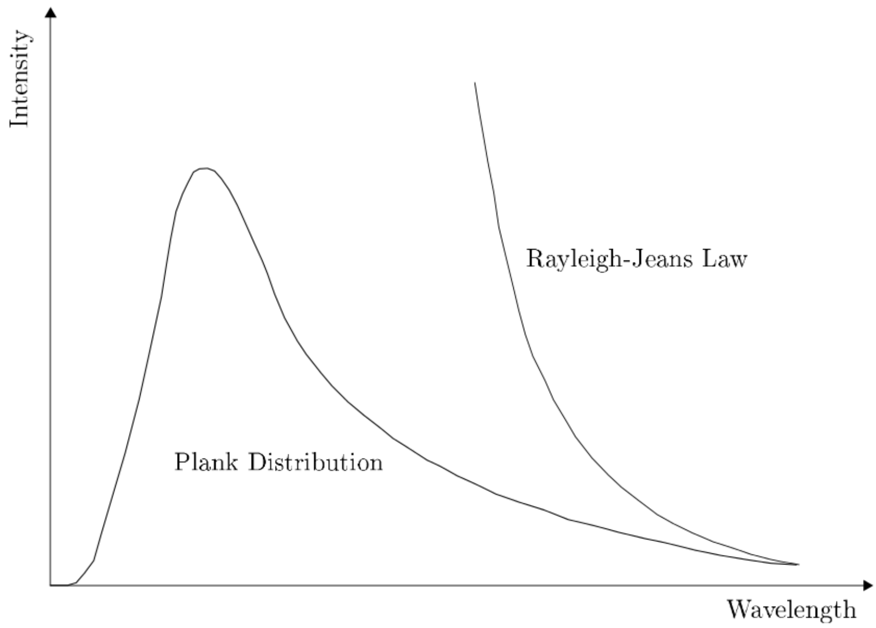

Figure 3.3: A diagram showing both the ideal Plank Distribution, and the Rayleigh-Jeans law that is valid in the high-wavelength limit

4. *Multiple Level Systems*

This chapter covers the basic concepts associated with multiple level systems, including the following:

- Molecules
- The Einstein Description
- Line Broadening
- Optical Gain
- Cavity Effects and Lasers

In the first two chapters, we spent our time looking at the quantum mechanical intricacies of atomic structure. Now, we are going to take a step back, and look at a more macroscopic view of transitions and energy levels. While quantum mechanics will still be a consideration in our analysis, the material involved in this chapter is for the most part semi-classical.

4.1 Molecules

Let us consider diatomic molecules, such that there is always rotational symmetry about the axis joining the the two constituent atoms. As the atoms are brought close together, the electrons in closed shells will usually remain in closed shells, and thus we will further restrict our consideration to valence electrons. At the characteristic scales of the molecule, the valence electrons can no longer be associated with a single nucleus, and are instead distributed throughout the molecule. The distribution of these electrons will determine whether the molecule remains bound, and if so, the resultant characteristics of the molecule.

4.1.1 Order of Magnitude Estimates

To get an idea of the energies that we are dealing with when it comes to molecules, we shall made order of magnitude estimates for the associated electronic, vibrational and rotational energies. A more exact calculation of the energy levels shall be performed in section 4.1.2.

Electronic Energy

Suppose that a given valence electron is confined to a region of size a. Then from the Uncertainty Principle:

$$\Delta x \Delta p \geq \frac{\hbar}{2} \quad \longrightarrow \quad p \backsim \frac{\hbar}{a} \tag{4.1}$$

We expect the electronic energy E_e to be of the same order of magnitude as the kinetic energy of the electrons. Hence

$$E_e \backsim \frac{p^2}{2m_e} = \frac{\hbar^2}{2m_e a^2} \tag{4.2}$$

Taking $a \backsim a_0$, it can be shown that E_e is roughly on the order of eV. We can also associated a time-scale with this energy of $\tau_e = \hbar / E_e$.

Vibrational Energy

We shall assume that the molecule can be treated as a classical harmonic oscillator around the centre of mass of the system. We define the reduced mass

$$\mu = \frac{m_1 m_2}{m_1 + m_2} \tag{4.3}$$

where m_1 and m_2 are the masses of the two nuclei. The potential energy associated with such an oscillator is then given by

$$V_{\text{vib}}(x) = \frac{1}{2}\mu\omega_{\text{vib}}^2 x^2 \tag{4.4}$$

We can argue that at $x \backsim a$, all of the electronic (kinetic) energy has to be vibrational $\langle V_{vib}(a)\rangle \backsim E_e$, allowing us to write that

$$\frac{1}{2}\mu\omega_{\text{vib}}^2 a^2 \backsim \frac{\hbar^2}{2m_e a^2} \quad \longrightarrow \quad \omega_{\text{vib}} \backsim \left(\frac{\hbar^2}{\mu m_e a^4}\right)^{1/2} \tag{4.5}$$

This means that the energy of the oscillator is given by

$$E_{\text{vib}} \backsim \sqrt{\frac{m_e}{\mu}} E_e \tag{4.6}$$

This means that the vibrational energies are smaller than the electronic energy by a factor of order $\sqrt{m/\mu} \backsim 100$.

Rotational Energy

If the nuclei rotate around their common centre of mass, then we can approximate the motion as a rigid rotor. We can ignore components of rotation that are about the internuclear axis, as these have a small moment of inertia. This means that we are left with contributions perpendicular to the internuclear axis, whose moment of inertia is given by $I = \mu a^2$. $\hbar$ is the typical scale of angular momentum, allowing us to write that

$$L \backsim I\omega_{\text{rot}} \backsim \hbar \quad \longrightarrow \quad \omega_{\text{rot}} \backsim \frac{\hbar}{I} \backsim \frac{\hbar}{\mu a^2} \tag{4.7}$$

The associated rotational energy is then given by

$$E_{\text{rot}} = \frac{1}{2} I \omega_{\text{rot}}^2 \backsim \frac{m}{\mu} E_e \tag{4.8}$$

The rotational energies are thus another factor of $\sqrt{m/\mu}$ smaller than E_e. We can thus write the following ordering of magnitudes and time-scales:

$$E_e \gg E_{\text{vib}} \gg E_{\text{rot}} \tag{4.9}$$

$$\tau_e \ll \tau_{\text{vib}} \ll \tau_{\text{rot}} \tag{4.10}$$

4.1.2 The Born-Oppenheimer Approximation

Now that we have gained some knowledge about the order of magnitudes of the energies associated with our system, we shall now calculate a more exact expression for these energy levels. Consider the Hamiltonian

$$H_{\text{molecular}} = \underbrace{T_n}_{\text{KE of nuclei}} + \underbrace{T_e}_{\text{KE of electrons}} + \underbrace{V(\mathbf{r}_i, \mathbf{R})}_{\text{potential energy}} \tag{4.11}$$

We can write these terms explicitly as

$$T_n = -\frac{\hbar^2}{2\mu}\nabla^2_{\mathbf{R}}, \quad T_e = -\sum_i^N \frac{\hbar^2}{2m_e}\nabla^2_{\mathbf{r}_i} \tag{4.12}$$

$$V(\mathbf{r}_i, \mathbf{R}) = \underbrace{\sum_j^2 \sum_i^N \left(-\frac{Z_j e^2}{4\pi\epsilon_0 \left|\mathbf{r}_i - \mathbf{R}_j\right|} \right)}_{\text{electron-nuclear interaction}} + \underbrace{\sum_{i<j}^N \frac{e^2}{4\pi\epsilon_0 |\mathbf{r}_i - \mathbf{r}_j|}}_{\text{electron-electron repulsion}} + \underbrace{\frac{Z_1 Z_2 e^2}{4\pi\epsilon_0 |\mathbf{R}|}}_{\text{internuclear repulsion}} \tag{4.13}$$

where $\mathbf{R}_1$ and $\mathbf{R}_2$ are the positions of the nuclei with respect to their centre of mass. We have moved the origin of our coordinate system to the centre of mass of the two nuclei, meaning that we describe their motion by a single particle of mass μ located at a position $\mathbf{R}$. The TISE for the system now reads

$$H_{\text{molecular}} \left|\Psi\right\rangle = E \left|\Psi\right\rangle, \quad \langle \mathbf{x}|\Psi\rangle = \Psi(\mathbf{r}_i, \mathbf{R}) \tag{4.14}$$

We shall attempt to find solutions for the molecular wave-function which are of the form of a product state

$$\left|\Psi\right\rangle = \left|\psi_n\right\rangle \left|\psi_e\right\rangle, \quad \text{or} \quad \Psi(\mathbf{r}_i, \mathbf{R}) = \psi_n(\mathbf{R})\psi_e(\mathbf{r}_i, \mathbf{R}) \tag{4.15}$$

where $\left|\psi_e\right\rangle$ satisfies the equation

$$H_e \left|\psi_e\right\rangle = E_e \left|\psi_e\right\rangle, \quad \langle \mathbf{x}|\psi_e\rangle = \psi_e(\mathbf{r}_i, \mathbf{R}) \tag{4.16}$$

where $H_e = T_e + V(\mathbf{r}_i, \mathbf{R})$. The above equation is most easily solved in a body-fixed coordinate system centred on the centre of mass, and orientated with the z-axis along $\mathbf{R}$; it is clear that in this coordinate system, the electronic energy E_e depends on the magnitude $R = |\mathbf{R}|$. However, it is important to remember that the wave-function $\psi_e(\mathbf{r}_i, \mathbf{R})$ is still *parametrised* by $\mathbf{R}$, as in the lab frame the origin of this body-fixed coordinate system will change based on the motion of the nuclei.

We now substitute (4.15) into (4.14):

$$[T_n + H_e] |\psi_n\rangle |\psi_e\rangle = E |\psi_n\rangle |\psi_e\rangle \tag{4.17}$$

Multiplying throughout by $\langle\psi_e|$, and integrating over the electron coordinate:

$$\langle\psi_e| T_n + H_e |\psi_e\rangle |\psi_n\rangle = E |\psi_n\rangle \quad \longrightarrow \quad \{\langle\psi_e| T_n |\psi_e\rangle + E_e(R)\} |\psi_n\rangle = E |\psi_n\rangle \tag{4.18}$$

where the second expression follows from (4.16). We now make the *Born-Oppenheimer approximation* that the electronic wavefunction has weak dependence on the magnitude R of the internuclear separation. This means that only the angular part of T_n acts on $|\psi_e\rangle$, allowing us to write that

$$\boxed{\begin{aligned} H_e |\psi_e\rangle &= E_e |\psi_e\rangle \\ \left[-\frac{\hbar^2}{2\mu R^2}\frac{\partial}{\partial R}\left(R^2\frac{\partial}{\partial R}\right) + \frac{\langle\psi_e| \mathbf{N}^2 |\psi_e\rangle}{2\mu R^2} + E_e(R)\right] |\psi_n\rangle &= E |\psi_n\rangle \end{aligned}} \qquad \begin{aligned}(4.19)\\(4.20)\end{aligned}$$

where $\mathbf{N}$ is the orbital angular momentum operator of the nuclei. We have thus reduced the problem to a system of two equations. In principle, the first can be solved for the electronic energy $E_e(R)$, where $|\psi_e\rangle$ is assumed to depend only weakly on the magnitude of $\mathbf{R}$, and depends on its *orientation* through a rotation of the coordinate system. The second can then be solved for the total energy E, where the electronic energy $E_e(R)$ acts as an effective potential for the nuclei.

Rotational and Vibrational Energies

Let us define the total orbital angular momentum of both the electrons and the nuclei as

$$\mathbf{K} = \mathbf{N} + \mathbf{L} \tag{4.21}$$

In the absence of any external torques, both $\mathbf{K}^2$ and K_z must commute with $H_{\text{molecular}}$, and so we can write the eigenvalue equations

$$\mathbf{K}^2 |\Psi\rangle = K(K+1)\hbar^2 |\Psi\rangle \tag{4.22}$$

$$K_z |\Psi\rangle = M_K \hbar |\Psi\rangle \tag{4.23}$$

Due to rotational symmetry about the internuclear axis, L_z is a constant of motion. $\mathbf{N}$ is perpendicular to $\mathbf{R}$ by definition, meaning that $K_z = L_z = \Lambda\hbar$ (note that the convention in molecular physics is to write $M_L = \Lambda$). Since the magnitude of $\mathbf{K}$ cannot be smaller than K_z, the smallest value of the total orbital angular momentum quantum number, K, is Λ. This means that $K = \Lambda, \Lambda+1, \Lambda+2, \ldots$.

The energy of the rotational motion of the nuclei moving in the potential $E_e(R)$ is given by the second term in (4.20). To evaluate $\langle\psi_e| \mathbf{N}^2 |\psi_e\rangle$, we note that

$$\mathbf{N^2} = \mathbf{K}^2 - \mathbf{L}^2 - 2\mathbf{N}\cdot\mathbf{L} \tag{4.24}$$

Since the electron angular momentum $\mathbf{L}$ precesses rapidly around the internuclear axis, the only non-zero time-averaged component of $\mathbf{L}$ is L_z, meaning that

$$\langle\psi_e|\,\mathbf{N}\cdot\mathbf{L}\,|\psi\rangle = 0 \quad \text{and} \quad \langle\psi_e|\,\mathbf{L}^2\,|\psi_e\rangle = \langle\psi_e|\,L_z^2\,|\psi_e\rangle = \Lambda^2\hbar^2 \tag{4.25}$$

This means that the rotational energy term becomes

$$\frac{\langle\psi_e|\,\mathbf{N}^2\,|\psi_e\rangle}{2\mu R^2} = \frac{\hbar^2}{2\mu R^2}\left[K(K+1)-\Lambda^2\right] \tag{4.26}$$

Now, since $E_e(R)$ is spherically symmetric, we can write the molecular wavefunction in the form

$$\langle\mathbf{x}|\psi_n\rangle = \psi_n(\mathbf{R}) = \psi_{\text{vib}}(R)\psi_{\text{rot}}(\Theta,\Phi) \tag{4.27}$$

where Θ and Φ are the angular coordinates associated with lab coordinate system, rather than the body centred coordinate system used to solve (4.19). In a similar fashion to section 1.1.1, we can separate the angular and radial equations, noting now that

$$K^2\psi_{\text{rot}}(\Theta,\Phi) = K(K+1)\hbar^2\,\psi_{\text{rot}}(\Theta,\Phi) \tag{4.28}$$

$$K_z\psi_{\text{rot}}(\Theta,\Phi) = M_K\hbar\,\psi_{\text{rot}}(\Theta,\Phi) \tag{4.29}$$

It thus follows that we can write

$$\left[-\frac{\hbar^2}{2\mu}\frac{\partial^2}{\partial R^2} + V_{\text{eff}}(R)\right]\psi_{\text{vib}}(R) = E\psi_{\text{vib}}(R) \tag{4.30}$$

where

$$\boxed{V_{\text{eff}}(R) = E_e(R) + \frac{\left[K(K+1)-\Lambda^2\right]\hbar^2}{2\mu R^2}} \tag{4.31}$$

is the *effective potential* for this one-dimensional Schrödinger equation.

The Effective Potential

For any bound state, we can expand $E_e(R)$ around its minimum value R_0:

$$E_e(R) = E_e(R_0) + \cancel{\left.\frac{dE_e}{dR}\right|_{R_0}(R-R_0)} + \frac{1}{2!}\left.\frac{d^2E_e}{dR^2}\right|_{R_0}(R-R_0)^2 + \dots \tag{4.32}$$

The second term is zero by definition of the minimum. Letting

$$K_s = \left.\frac{d^2E_e}{dR^2}\right|_{R_0} \quad \text{and} \quad B_r = \frac{\hbar^2}{2\mu R_0^2} = \frac{\hbar^2}{2I_M} \tag{4.33}$$

we can approximate the value of the effective potential around the equilibrium value R_0 as

$$V_{\text{eff}}(R) \backsim E_e(R_0) + B_rK(K+1) + \frac{1}{2}K_s(R-R_0)^2 \tag{4.34}$$

where we have absorbed the $\Lambda^2\hbar^2/2\mu R_0^2$ term into $E_e(R_0)$. It thus becomes clear that V_{eff} has the form of a harmonic potential raised by a constant energy $E_e(R_0)+B_rK(K+1)\hbar^2$. Thus, the eigenvalue solution to (4.30) is given by

$$\boxed{E = E_e(R_0) + \left(\nu+\frac{1}{2}\right)\hbar\omega_{\text{vib}} + B_rK(K+1), \quad \omega_{\text{vib}} = \left(\frac{K_s}{\mu}\right)^{1/2}} \tag{4.35}$$

The effect of the electronic energy on the nuclei can be modelled via the Morse potential

$$E_e(R) = A\left[1 - e^{-B(R-R_0)}\right]^2 \tag{4.36}$$

where A and B are constants, and R_0 is the equilibrium separation of the two molecules when rotational energy levels are not excited. Derive an expression for ω_{vib}. Suppose now that the molecule is rotating. Derive an expression for the new equilibrium distance between the two molecules, and calculate the resultant shift in energy.

As anticipated by (4.32), we expand the Morse potential around the equilibrium position R_0:

$$E_e(R) \backsim A\left[B^2(R-R_0)^2 - B^3(R-R_0)^3 + \dots\right] \tag{4.37}$$

We can then equate the quadratic term to the harmonic oscillator potential:

$$AB^2(R-R_0)^2 = \frac{1}{2}\mu\omega_{\text{vib}}^2(R-R_0)^2 \quad \longrightarrow \quad \omega_{\text{vib}} = \left(\frac{2A}{\mu}\right)^{1/2} B \tag{4.38}$$

In the case that the rotational energy levels become excited, we can write the energy of the system as

$$E = A\left[1 - e^{-B(R-R_0)}\right]^2 + \frac{K(K+1)\hbar^2}{2\mu R^2} \tag{4.39}$$

Evidently, this has shifted the potential curve, and thus the minimum of the system. We thus can find the new equilibrium by finding the minimum of this equation. Differentiate with respect to R, and then let $R = R_0 + \delta R$ to obtain:

$$2AB\left(1 - e^{-B\delta R}\right)e^{-B\delta R} = \frac{K(K+1)\hbar^2}{\mu(R_0+\delta R)^3} = \frac{K(K+1)\hbar^2}{\mu R_0^3}\left(1 + \frac{\delta R}{R_0}\right)^{-3} \tag{4.40}$$

Expanding to leading order in δR, we find that

$$\delta R = \frac{K(K+1)\hbar^2}{2\mu AB^2R_0^3} \quad \longrightarrow \quad R = R_0\left(1 + \frac{K(K+1)\hbar^2}{2\mu AB^2R_0^4}\right) \tag{4.41}$$

Calculating the resultant shift in energy is actually a more involved task than it initially appears. A naive approach would involve substituting the result for the new equilibrium into (4.39). However, one should actually expand (4.39) around the new equilibrium position $R = R_0 + \delta R$. This is because the shift in R is non-trivial, and will actually modify the effective spring constant of the system; in other words, there will be a non-negligible contribution to the shift from the vibrational energy. Taking the naive approach would only find the shift due to the electronic and rotational energies, and not the vibrational energies.

4.1.3 Symmetry and Energy Levels

For individual atoms, there is no unique special axis that we can associate with the system, meaning that the system is spherically symmetric, and $\mathbf{L}^2$ is a constant of the motion. However, in a molecule, the internuclear axis is an obvious special axis of the system, which breaks our spherical symmetry. As alluded to in section 4.1.2, this means that $\mathbf{L}^2$ is no longer a constant of motion; instead, we choose to align our z-axis along $\mathbf{R}$, meaning that L_z is a constant of motion. We thus characterise our states by Λ, instead of L as before.

As in atoms, we can also associate the total spin $\mathbf{S} = \sum_i \mathbf{s}_i$ with the electrons. These have no coupling to the electric field along the internuclear axis, and so the total spin is calculated in the same way as for the atom. Like in atomic structure, the spin state of the system has an effect on the spatial wave-function due to symmetry considerations, and thus on the energy of the system. We thus also have to specify the total spin S of the system when labelling our states.

For any diatomic molecule, H_e is unaffected by a reflection of the coordinate system in a plane that contains the internuclear axis due to rotational symmetry around said axis. Let $A_{\mathbf{R}}$ be the operator corresponding to such a reflection. It can be shown that

$$A_{\mathbf{R}}L_z = -L_z A_{\mathbf{R}} \quad \longrightarrow \quad [A_{\mathbf{R}}, L_z] \neq 0 \quad \text{if} \quad L_z \neq 0 \tag{4.42}$$

This means that we can only form simultaneous eigenfunctions of $A_{\mathbf{R}}$, L_z and H_e for $\Lambda = 0$, giving rise to two generate states labelled by $\pm$.

Homonuclear molecules are those that contain a single type of nucleus. These have an addition centre of symmetry at the centre of mass of the system, meaning that H_e remains unchanged under parity inversion $\mathcal{P}[\mathbf{r}_i \to -\mathbf{r}_i]$. In homonuclear molecules, we label the states 'g' (gerade) if the electronic wavefunction does not change sign under $\mathcal{P}$, and 'u' (ungerade) if the wavefunction does change sign.

With these symmetry considerations outlined, we can now write a spectroscopic notation to denote our molecular energy levels, as shown in figure 4.1.

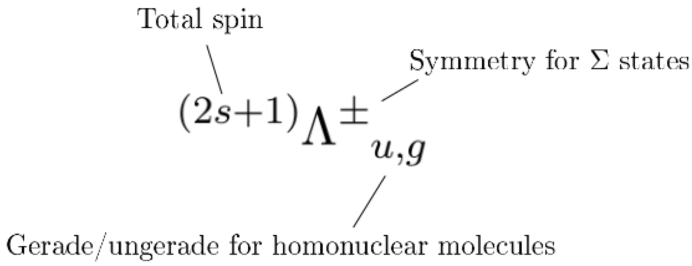

Figure 4.1: Notation for electronic molecular states

The values of Λ are notated by Σ, Π, Δ, Φ for $\Lambda = 0, 1, 2, 3, \dots$ for the electronic states.

4.1.4 Molecular Selection Rules

Under the electric dipole approximation (see section 3.1.1), the transition rates are proportional to

$$|D_{21}|^2 = \left|\langle\Psi| - \mathbf{D}\cdot\widehat{\mathbf{E}}\left|\Psi'\right\rangle\right|^2 \tag{4.43}$$

where the single prime indicates the lower energy level respectively. $\widehat{\mathbf{E}}$ is a unit vector pointing in the direction of the radiation, and we define the *dipole operator* as

$$\mathbf{D} = eZ_1\mathbf{R}_1 + eZ_2\mathbf{R}_2 - e\sum_i \mathbf{r}_i = \mathbf{D}_n + \mathbf{D}_e \tag{4.44}$$

When writing the integral expression for D_{21}, we once again make the Born-Oppenheimer approximation that the electronic wavefunctions are slow functions in $\mathbf{R}$, meaning that we can evaluate the electronic integral around $\mathbf{R} = \mathbf{R}_0$. Then:

$$D_{21} \backsim \underbrace{\int d\tau_e \, \psi_e^*(\mathbf{r}_i, \mathbf{R}_0)\mathbf{D}\psi_{e'}(\mathbf{r}_i, \mathbf{R}_0)}_{\text{electronic, } I_e} \underbrace{\int dR \, \psi_{\text{vib}}^*(R)\psi_{\text{vib}'}}_{\text{vibrational, } I_{\text{vib}}} \times \underbrace{\int d\Theta d\Phi \, \sin\Theta \, \psi_{\text{rot}}^*(\Theta, \Phi)\mathbf{D} \cdot \widehat{\mathbf{E}}\psi_{\text{rot}'}(\Theta, \Phi)}_{\text{rotational, } I_{\text{rot}}} \tag{4.45}$$

We can use this expression to motivate the selection rules associated with molecular transitions. Evidently, if any part of this integral evaluates to zero, then the transition is forbidden under the electric dipole approximation.

Transitions with no change of electronic states

Transitions of this type are only involved in heteronuclear molecules, since for homonuclear molecules the I_e is zero as $\mathbf{D}_n = 0$ as $\mathbf{R}_1 = -\mathbf{R}_2$, and $\mathbf{D}_e$ makes no contribution to the integral as it is of definite parity.

If the Born-Oppenheimer approximation holds rigorously, then transitions involving a change in both the rotational and vibrational quantum numbers is forbidden, since within a given electronic state, the vibrational wavefunctions are zero, forcing $I_{\text{vib}} = 0$. However, in practise, I_e is not independent of $\mathbf{R}$; if on expands the integral around $\mathbf{R} = \mathbf{R}_0$, an extra term is introduced. This gives rise to the selection rules:

$$\boxed{\begin{aligned} &|K - K'| \leq 1 \quad \text{except } |K - K'| \neq 0 \text{ for } \Lambda = \Lambda' = 0 \\ &|\nu - \nu'| = 1 \end{aligned}} \qquad (4.46),\ (4.47)$$

Transitions with a change of electronic state

If the transition involves a change in electronic state, then I_e can be nonzero for both homonuclear and heteronuclear molecules, as the wavefunctions $\psi_e(\mathbf{r}_i, \mathbf{R}_0)$ and $\psi_{e'}(\mathbf{r}_i, \mathbf{R}_0)$ will be distinct. In this case, we retain the selection rules above, except now we have the additional rules:

$$\boxed{\begin{aligned} |S - S'| &= 0 \\ |\Lambda - \Lambda'| &\leq 1 \\ \Sigma^{\pm} &\rightarrow \Sigma^{\pm} \\ g &\rightarrow u \end{aligned}} \qquad (4.48)\text{–}(4.51)$$

where the last two apply to Σ states and homonuclear molecules respectively. It is clear that the symmetry associated with Σ cannot change under a transition, while homonuclear molecules must undergo a parity inversion.

4.2 The Einstein Description

We are now going to treat the interaction of radiation and matter via what is known as the *Einstein description*, as this will give us a basis from which to tackle more complicated systems, such as lasers. This description considers two atomic energy levels, the upper level having energy E_2 and the lower level having energy E_1, with degeneracies g_2 and g_1 respectively. Each level as an atomic *population per unit volume* n_2 and n_1 respectively, with associated *florescence lifetimes* τ_2 and τ_1 (against all types of decay). We further define a characteristic timescale $\omega_{21}^{-1} = \hbar/(E_2 - E_1)$ associated with transitions between these energy levels.

4.2.1 Einstein Coefficients

We can identify three processes by which radiation can interact with an atom in these levels, as follows:

- Spontaneous emission - An atom in the upper level decays to the lower level by the mission of a photon with energy $\hbar\omega_{21}$. The rate per unit volume at which this spontaneous decay occurs can be written as $n_2 A_{21}$. It is clear that A_{21} defines some characteristic rate for the transition, meaning that for a closed system of only two levels, $A_{21} \backsim \tau_2^{-1}$
- Absorption - An atom in the lower level is excited to the upper level by absorption of a photon of energy $\hbar\omega_{21}$. The rate per unit volume at which this excitation occurs is given by $n_1 B_{12}\rho(\omega_{21})$, where $\rho(\omega_{21})$ is the spectral energy density associated with radiation of an angular frequency ω_{21}, and B_{12} is a constant characteristic of the transition
- Stimulated emission - An incident photon of energy $\hbar\omega_{21}$ stimulates an atom in the upper level to decay into the lower level by the re-emission of a photon of energy $\hbar\omega_{21}$. The emitted photon has the same direction and polarisation as the incident photon. The rate at which this occurs is given by $n_2 B_{21}\rho(\omega_{21})$, where $\rho(\omega_{21})$ is as before, and B_{21} is a constant characteristic of the transition

The coefficients A_{21}, B_{12} and B_{21} are known as the *Einstein A and B coefficients.* Together, these characterise the transition rates for a given two-level system.

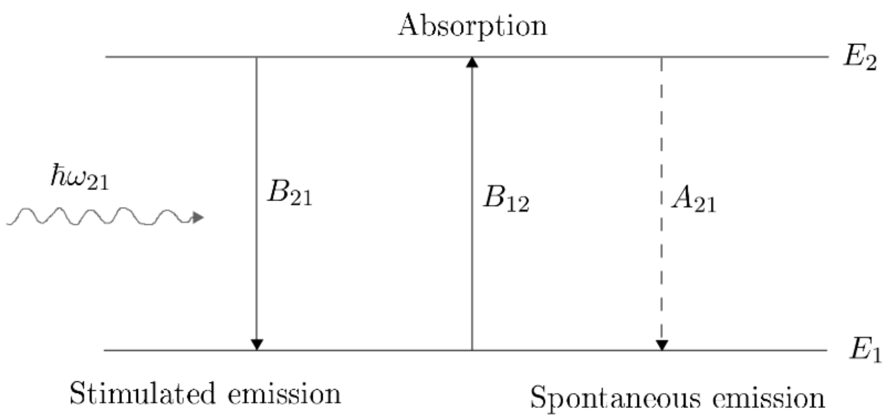

Figure 4.2: Absorption and emission in a two level system, showing the relevant Einstein coefficients

By energy conservation, the rate of absorption has to be equal to the rate of emission (of both types), allowing us to write that

$$n_1 B_{12}\rho(\omega_{21}) = n_2 A_{21} + n_2 B_{21}\rho(\omega_{21}) \tag{4.52}$$

We can re-arrange this expression for the spectral energy density:

$$\rho(\omega_{21}) = \frac{A_{21}}{\frac{n_1}{n_2}B_{12} - B_{21}} \tag{4.53}$$

Now, we argue that in thermal equilibrium, the spectral energy density can be approximated by the Plank distribution (3.50), while the individual populations will have Boltzmann-like distributions, such that

$$\frac{n_1}{n_2} = \frac{g_1}{g_2}e^{\beta\hbar\omega_{21}} \quad \longrightarrow \quad \rho(\omega_{21}) = \frac{A_{21}}{B_{21}}\frac{1}{\frac{g_1 B_{12}}{g_2 B_{21}}e^{\beta\hbar\omega_{21}} - 1} \tag{4.54}$$

Comparison with (3.50) yields the following relationships between the Einstein coefficients:

$$\boxed{g_1 B_{12} = g_2 B_{21}, \quad A_{21} = \frac{\hbar\omega_{21}^3}{\pi^2 c^3}B_{21}} \tag{4.55}$$

While this derivation assumed that the spectral energy density was a Plank distribution, these relationships hold for *any* radiation field. This is because these relationships do not depend on the specific form of the field, as the coefficients are properties of the atoms themselves, rather than the radiation field.

We are actually able to find explicit expressions for the Einstein coefficients under the electric dipole approximation. Let R_{12} be the rate of absorption between the two levels due to the incoming radiation. Then, it is clear that $R_{12} = B_{12}\rho(\omega_{21})$. Comparison of this expression with (3.12) then yields the fact that

$$\boxed{B_{12} = \frac{2\pi e^2}{3\epsilon_0\hbar^2}|\langle m| z |n\rangle|^2} \tag{4.56}$$

The other coefficients can then be found by making use of the relationships in (4.55).Note that $\langle m| z |n\rangle \backsim a_0$.

Now, let us suppose that we have an atom with many energy levels. There will obviously be transitions possible between any two energy levels within the ladder, meaning that the steady state condition for the entire atom is significantly more complicated than (4.52). However, the simplest way of ensuring that the entire atom remains in dynamical equilibrium is to assume that any pair of levels must be in thermal equilibrium with one another, as this forces all other pairs to be in thermal equilibrium with one another. This statement is known as *detailed balance*. It is thus not necessary to assume that the atom only has two levels.

4.2.2 Population Inversion

As we will see more formally later, for light amplification by the stimulated emission of radiation (laser) we require the rate of stimulated emission to be greater than the rate of absorption. This gives the condition for optical gain as

$$\boxed{\frac{n_2}{g_2} > \frac{n_1}{g_1}} \tag{4.57}$$

That is, the population per state must be greater in the upper level than the lower level. This is known as *population inversion*. However, for a system in thermal equilibrium, we know that the first expression in (4.54) must hold. This means that we cannot obtain a population inversion in thermal equilibrium.

We thus now ask the conditions under which a population inversion is actually possible. Let us introduce the *pump rates* R_2 and R_1 for the upper and lower levels respectively; these describe the rates at which atoms are supplied to each level. In R_2, we include all the possible processes that may excite the upper level, including direct optical pumping, electron collisional excitation, and radiative and non-radiative cascade from higher lying levels. This is similar for R_1, except we choose to not include the spontaneous emission on the laser transition itself in R_1, and instead write it explicitly. We can then write the *rate equations*:

$$\frac{dn_2}{dt} = R_2 - \frac{n_2}{\tau_2} \tag{4.58}$$

$$\frac{dn_1}{dt} = R_1 + n_2 A_{21} - \frac{n_1}{\tau_1} \tag{4.59}$$

Solving these equations in the steady state, we find that

$$n_2 = R_2 \tau_2 \tag{4.60}$$

$$n_1 = R_1 \tau_1 + R_2 \tau_2 A_{21} \tau_1 \tag{4.61}$$

For population inversion, we require that (4.57) is satisfied. Subsisting these results in yields

$$\boxed{\frac{R_2}{R_1}\frac{\tau_2}{\tau_1}\frac{g_1}{g_2}\left(1 - \frac{g_2}{g_1}A_{21}\tau_1\right) > 1} \tag{4.62}$$

The factor in brackets above must be less than one, and can be negative, as well as positive, as it depends only on the parameters associated with the laser transition, rather than the pumping rates. This means that a *necessary, but not sufficient*, condition for achieving a steady state population inversion is

$$A_{21} < \frac{g_1}{g_2}\frac{1}{\tau_1} \tag{4.63}$$

Physically, this arises due to the fact that increasing the population of the upper level by increasing the rate of laser pumping also increases the rate at which the lower level is populated by spontaneous emission on the laser transition itself. Thus, to achieve a steady state population inversion, both the above condition and *at least* one of the following must be satisfied:

- Selective pumping $R_2 > R_1$ - The upper level is pumped more rapidly than the lower level
- Favourable lifetime ratio $\tau_2 > \tau_1$ - The lower level decays much more rapidly than the upper level, and so its small by comparison
- Favourable degeneracy ratio $g_1 > g_2$ - Ensures that the population per state of the lower level is small

This limits the range of transitions that can actually be used to laser excitation, as we will see later.

4.2.3 Rabi Oscillations

You can have Rabbi oscillations, but that requires two Jews and a see-saw
- Professor Simon Hooker

The term *Rabi oscillations* (pronounced "rah-bee") is used to refer to the oscillation of the atomic population between the two levels of a two-level system at some characteristic frequency. Let us label our eigenstates of our two-level system by $|1\rangle$ and $|2\rangle$. Suppose that monochromatic light of amplitude $\mathbf{E}_0$ and frequency ω is incident on the atom, such that we can write a time-dependent perturbation

$$\delta H(t) = e\mathbf{x} \cdot \mathbf{E}_0 \cos \omega t \tag{4.64}$$

We can the write the overall state of our system as

$$|\psi, t\rangle = c_1 e^{-iE_1 t/\hbar} |1\rangle + c_2 e^{-iE_2 t/\hbar} |2\rangle \tag{4.65}$$

where the time evolution of the coefficients amplitudes c_1 and c_2 are given by (3.4)

$$\dot{c}_2 = -\frac{i}{\hbar} \langle 2| \delta H |1\rangle c_1 e^{i\omega_0 t}, \quad \dot{c}_1 = -\frac{i}{\hbar} \langle 1| \delta H |2\rangle c_2 e^{-i\omega_0 t} \tag{4.66}$$

where $\omega_0 = \omega_{21}$. Let δH_{ij} represent the entries of the matrix corresponding to the perturbation δH. If we assume δH is real - which is a valid thing to do as it represents a measurable quantity - then it is clear that the matrix must be Hermitian, such that $\delta H_{12}^* = \delta H_{21} \longrightarrow \delta H_{12} = \delta H_{21}$. The fact that $\delta H_{11} = \delta H_{22} = 0$ follows from the fact that $\mathbf{x}$ has odd parity, while our basis states $|1\rangle$ and $|2\rangle$ are of even parity, forcing the matrix elements to be zero. We can thus write our matrix element as

$$\delta H_{12} = \frac{\hbar\Omega}{2}\left(e^{i\omega t} + e^{-i\omega t}\right) \quad \text{for} \quad \boxed{\Omega = \frac{1}{\hbar} \langle 1| e\mathbf{x} \cdot \mathbf{E}_0 |2\rangle} \tag{4.67}$$

The quantity Ω is the Rabi frequency that is associated with the oscillations; it is clear that this increases with the strength of the electric field. This allows us to write the time evolution of c_2 as

$$\dot{c}_2 = -\frac{i\Omega}{2} c_1 \left(e^{i(\omega+\omega_0)t} + e^{i(\omega_0-\omega)t}\right) \tag{4.68}$$

We now make what is known as the *rotating wave approximation*, by assuming that the frequency of the electric field perturbation is close to the atomic resonance ω_0. That is, $\omega = \omega_0 + \delta\omega$, where $\delta\omega \ll \omega_0$. Then, we have that

$$|\omega - \omega_0| \ll \omega_0 \quad \text{and} \quad \omega + \omega_0 \backsim 2\omega_0 \tag{4.69}$$

This means that we can ignore the fast oscillating term $\omega + \omega_0$ in comparison to $\omega - \omega_0$, as the oscillations associated with the former will average to zero over the time scales associated with the latter. Thus, neglecting the $\omega + \omega_0$ terms in (4.66), we can write

$$\dot{c}_2 = -\frac{i\Omega}{2} c_1 e^{-i\delta\omega t}, \quad \dot{c}_1 = -\frac{i\Omega}{2} c_2 e^{i\delta\omega t} \tag{4.70}$$

Recalling the fact that both the exponential factor and the coefficients are time dependent, we can solve this coupled system to obtain a second order differential equation for c_2 (or alternatively c_1):

$$\ddot{c}_2 - i\delta\omega\, \dot{c}_2 + \left|\frac{\Omega}{2}\right|^2 c_2 = 0 \tag{4.71}$$

Suppose that the initial state of the system is $|\psi, 0\rangle = |1\rangle$. Then, the resultant solution for the probability associated with c_2 is given by

$$|c_2(t)|^2 = \frac{\Omega^2}{\Omega^2 + \delta\omega^2} \sin^2\left(\frac{1}{2}t\sqrt{\Omega^2 + \delta\omega^2}\right) \tag{4.72}$$

The amplitude can be found by substitution of the general solutions into (4.70), or by recognising that it must reduce to one for $\delta\omega \to 0$. We have found the steady-state solution in the ideal case; the atomic population simply oscillates back and forth between the two levels. However, in reality, these oscillations will be damped, resulting in static, steady state populations predicted by the rate equations (4.58) and (4.59). The timescale of the damping will be roughly τ_2, as this controls the rate of spontaneous emission from the upper level. It is clear that in order to observe Rabi oscillations, we require that $\Omega \gg \tau_2^{-1}$.

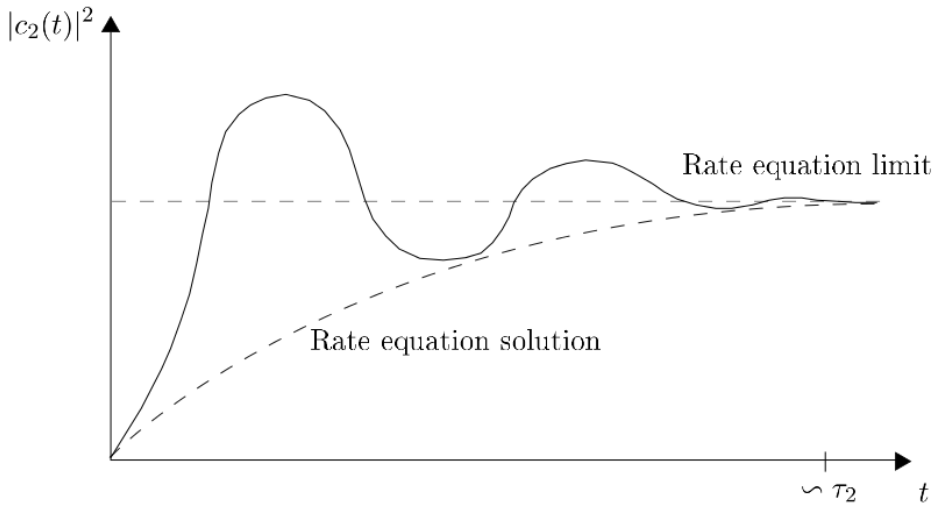

Figure 4.3: The time evolution of $|c_2(t)|^2$ with damping present

It is clear that the evolution of the population that is predicted by the rate equations does not display the physics associated with Rabi-oscillations.

The Bloch Sphere

A useful way to visualise the time evolution of such as system is through the use of the *Bloch sphere*. This is a geometrical representation of the pure state space of a two-level quantum mechanical system on which the *Bloch vector* moves. The direction in which the Bloch vector points is indicative of the relative occupation of the two levels associated with the system. It is defined by the coordinates (θ, ϕ), and is defined such that

$$\boxed{c_1 = \cos\frac{\theta}{2}, \quad c_2 = e^{i\phi}\sin\frac{\theta}{2}} \tag{4.73}$$

Using these definitions of c_1 and c_2 in (4.65), we can write that

$$|\psi, t\rangle = e^{-iE_1 t/\hbar}\left(\cos\frac{\theta}{2}|1\rangle + e^{i\phi - i\omega_0 t}\sin\frac{\theta}{2}|2\rangle\right) \tag{4.74}$$

We are at liberty to choose the phase $\phi = \omega_0 t$ (for example), such that we sit in a rotating frame where all the dynamics is described by θ. In this case, the vertical (z) component of the Bloch vector represents the degree of atomic excitation.

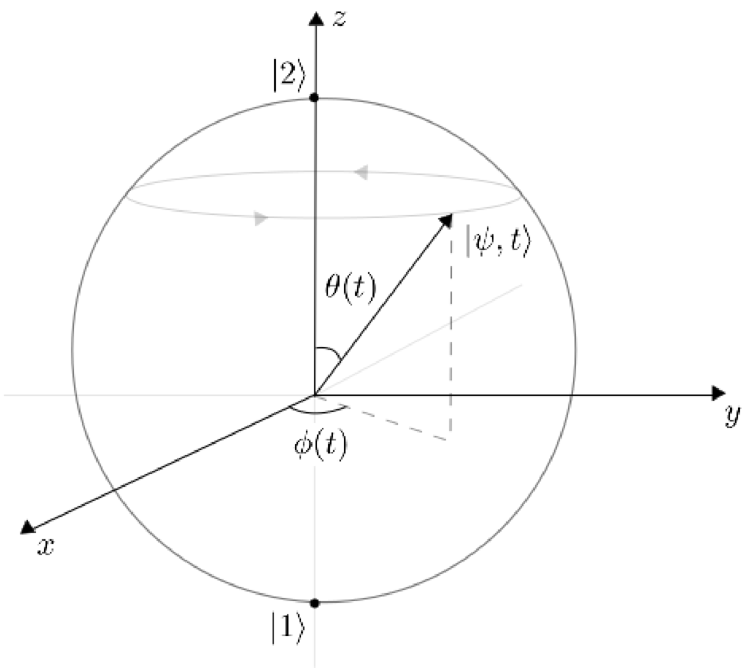

Figure 4.4: The Bloch sphere and Bloch vector in the pure state space of the system

Let us take a look at an example. Suppose that we are at resonance, such that $\delta\omega = 0$. Then, it is trivial to show that

$$c_1 = \cos\left(\frac{1}{2}\Omega t\right), \quad c_2 = i\sin\left(\frac{1}{2}\Omega t\right) \tag{4.75}$$

If we choose $\phi = \omega_0 t$, then it is easy to see that $\theta = \Omega t$. That is, the Bloch vector rotates around the x-axis at an angular frequency Ω, visiting the eigenstates $|1\rangle$ and $|2\rangle$ every half cycle.

In the absence of any external field, the Bloch vector will precess around z, corresponding the evolution of the phases of the states $|1\rangle$ and $|2\rangle$ in the steady state (ϕ has no dependence on E_0). This means that it is possible to perform a rotation about another axis by allowing the system to reach some superposition of states (eg. $t = \frac{\pi}{2\Omega}$), and then removing the external field. If the external field is then re-introduced, the precession induced due to the external field will be about another axis.

4.3 Line Broadening

Thus far, we have implicitly assumed that the frequencies involved in our transitions are monochromatic. However, this is evidently only an approximation; the transitions can be characterised by some *lineshape* function $g(\omega - \omega_0)$. It is normalised such that

$$\int_0^\infty d\omega \, g(\omega - \omega_0) = 1 \tag{4.76}$$

and has the property that it peaks around the transition frequency, as would be expected. There are various different factors that lead to line broadening, which we will detail in the following sections.

4.3.1 Homogeneous Broadening

A *homogeneous broadening* mechanism is one which affects all atoms in a sample equally, and consequently all atoms will interact with a beam of frequency ω with the same strength. This will generally produce a *Lorentzian* lineshape.

Natural Broadening

As we saw in section 4.2.3, we can associate a dipole moment $p(t) = p_0 \cos(\omega_0 t)$ with a two level system. Let $\mathcal{E}$ be the energy of the oscillations. Then, we know from Special Relativity that an oscillating dipole radiates away energy according to Larmor's formula (see B2 notes)

$$\mathcal{P}_L = \frac{\omega_0^4 p_0^2}{12\pi\epsilon_0 c^3} \tag{4.77}$$

We note that $\mathcal{E} \propto p_0^2$, meaning that we can write

$$\frac{d\mathcal{E}}{dt} = -\gamma\mathcal{E} \quad \longrightarrow \quad \mathcal{E} = \mathcal{E}(0)e^{-\gamma t} \tag{4.78}$$

for some constant of proportionality γ. As $\mathcal{E} \propto E_0^2$, it follows that the electric field associated with the dipole oscillation in the far field regime is given by

$$\mathbf{E}(t) = \mathbf{E}_0 \exp\left(-\frac{\gamma}{2}t\right) \sin\omega_0 t \tag{4.79}$$

The frequency distribution of this field will be given by the Fourier transform of $E(t)$; we see immediately that the spectrum will consist of a range of frequencies due to the fact that $\mathbf{E}$ is no longer a pure harmonic wave. The signal from a detection system able to measured the emitted spectrum will be proportional to the modulus-square of the resulting expression, giving us the associated lineshape

$$\boxed{g_L(\omega - \omega_0) = \frac{1}{\pi} \frac{\gamma/2}{(\omega - \omega_0)^2 + (\gamma/2)^2}} \tag{4.80}$$

This has associated full-width at half maximum (FWHM) of $\Delta\omega_N = \gamma$. This is known as the *natural* or*lifetime* broadened width. We can find an expression for broadening via uncertainty principle considerations:

$$\Delta E_1 \backsim \frac{\hbar}{\tau_1}, \; \Delta E_2 \backsim \frac{\hbar}{\tau_2} \quad \longrightarrow \quad \Delta E \backsim \hbar\left(\frac{1}{\tau_1} + \frac{1}{\tau_2}\right) \tag{4.81}$$

This allows us to conclude that

$$\boxed{\Delta\omega_N = \gamma = \frac{1}{\tau_1} + \frac{1}{\tau_2}} \tag{4.82}$$

Pressure Broadening

Another homogeneous broadening mechanism is that of pressure broadening. During the radiating time of an atom, a collision with another atom can take place, which may cause an electron to transition without radiating, as the excess energy is carried away by the other atom. As this applies to both levels, this causes another Lorentzian lineshape, except the FWHM has been modified to

$$\boxed{\Delta\omega_P = \gamma + \frac{2}{\tau_c}} \tag{4.83}$$

τ_c is the mean collision time for the atoms in the sample. We can approximate this via Kinetic theory:

$$\tau_c \backsim \frac{1}{\sigma_{12} n v_{th}}, \quad \sigma_{12} \backsim \pi(r_1^2 + r_2^2) \tag{4.84}$$

where r_1, r_2 are the atomic radii of the two species, if applicable.

4.3.2 Inhomogeneous Broadening

The effect of *inhomogeneous broadening* depends on the specific properties of the atoms involved: $\mathbf{r}$, $\mathbf{v}$, m .... The distribution of these different 'types' of atoms leads to an observed broadening when the emission or absorption of the whole sample is viewed. These will generally produce a *Gaussian* lineshape.

Doppler Broadening

The main inhomogeneous broadening mechanism is *Doppler broadening* due to the thermal motion of atoms inside the source. Suppose that we place our axis of observation along the z-axis. Let ω_0 be the transition frequency in the absence of the Doppler shift, and v_z be the component of the velocity of an atom in the source along z. Then, the Doppler shifted frequency ω is given by

$$\omega - \omega_0 = \frac{v_z}{c}\omega_0 \quad \longrightarrow \quad v_z = c\frac{\omega - \omega_0}{\omega_0} \tag{4.85}$$

We know from Kinetic theory that in equilibrium, the velocity distribution of the atoms in the source is given by

$$f(v_z)dv_z = \frac{1}{\sqrt{\pi}v_{th}} e^{-v_z^2/v_{th}^2}, \quad v_{th} = \sqrt{\frac{2k_BT}{m}} \tag{4.86}$$

Substitution of the second expression in (4.85) into (4.86) yields the lineshape function

$$\boxed{g_D(\omega - \omega_0) = \frac{1}{\Delta\omega_D/2}\sqrt{\frac{\log 2}{\pi}} \exp\left(-\left[\frac{\omega - \omega_0}{\Delta\omega_D/2}\right]^2 \log 2\right)} \tag{4.87}$$

This is a Gaussian distribution, with the associated FWHM frequency

$$\boxed{\Delta\omega_D = 2\sqrt{\log 2}\frac{v_{th}}{c}\omega_0} \tag{4.88}$$

This is known as the *Doppler width*. Generally, one finds that the magnitude of the homogeneous broadening is an order higher than that of the inhomogeneous broadening; this makes physical sense, as the former is a global effect, while the latter is not.

4.3.3 Line Broadening and the Einstein Coefficients

Now that we have made the admission that our transition frequency is not in fact a delta function, let us look at the effect that this has on our Einstein coefficients. Once again, we look at the three different processes, assuming that they are all homogeneously broadened:

- Spontaneous emission - The rate per unit volume, in the frequency range $[\omega, \omega + d\omega]$, at which this spontaneous decay occurs can be written as $n_2 A_{21} g_A(\omega - \omega_0) d\omega$, where $g_A(\omega - \omega_0)$ is the lineshape for spontaneous emission
- Absorption - The rate per unit volume, in the frequency range $[\omega, \omega + d\omega]$, at which this excitation occurs is given by $n_1 B_{12} g_B(\omega - \omega_0) \rho(\omega_{21}) d\omega$, where $g_B(\omega - \omega_0)$ is the lineshape for absorption.
- Stimulated emission - The rate at which this occurs is given by $n_2 B_{21} g_{B'}(\omega - \omega_0) \rho(\omega_{21}) d\omega$, where $\rho(\omega_{21})$ is as before, where $g_{B'}(\omega - \omega_0)$ is the lineshape for absorption.

Note that we have assumed that the lineshapes for each of the transitions are distinct. But how are they related? We can follow an identical method used in section 4.2.1 for a system in thermal equilibrium to show that

$$g_1 B_{12} g_B(\omega - \omega_0) = g_2 B_{21} g_{B'}(\omega - \omega_0) \tag{4.89}$$

$$A_{21} g_A(\omega - \omega_)) = \frac{\hbar \omega_0^3}{\pi^2 c^3} B_{21} g_{B'}(\omega - \omega_0) \tag{4.90}$$

As these expressions must be hold for all possible functions, it immediately follows from comparison with (4.55) that $g_A(\omega - \omega_0) = g_B(\omega - \omega_0) = g_{B'}(\omega - \omega_0)$. Thus, all of the transition types have a lineshape that is equal to some homogeneous lineshape function $g_H(\omega - \omega_0)$.

4.4 Optical Gain

We shall now investigate how a beam of radiation of spectral intensity $I(\omega, \mathbf{x})$ may be amplified as it passes through a medium.

Suppose, without loss of generality, that the beam propagates along the z-axis through a medium with population densities n_2 and n_1 in the upper and lower levels respectively. Let $\rho(\omega, z)$ be the spectral energy density of the radiation as before. Consider the beam travelling over the interval $[z, z + dz]$. The net rate at which atoms are transferred from the upper to the lower laser level by the stimulated emission of photons with frequencies in the range $[\omega, \omega + d\omega]$ is given by

$$[n_2 B_{21} - n_1 B_{12}] g_H(\omega - \omega_0)\rho(\omega, z) d\omega \qquad \underbrace{Adz}_{\text{volume of beam}} \tag{4.91}$$

Each transition releases an energy of $\hbar\omega$ to the beam, and so the power gain is

$$[n_2 B_{21} - n_1 B_{12}] g_H(\omega - \omega_0)\rho(\omega, z)\hbar\omega d\omega Adz \tag{4.92}$$

Alternatively, we can write the change in power of the beam with distance as

$$[I(\omega, z + dz) - I(\omega, z)]\, Ad\omega \tag{4.93}$$

Equating (4.92) and (4.93), and taking the limit as $dz \to 0$, it follows that

$$\frac{\partial I}{\partial z} = [n_2 B_{21} - n_1 B_{12}]\, g_H(\omega - \omega_0)\frac{\hbar\omega}{c} I(\omega, z) \tag{4.94}$$

where we have used the fact that for a beam of radiation $I(\omega, z) = \rho(\omega, z)c$. This result can be recast into the more useful form

$$\boxed{\frac{\partial I}{\partial z} = n^* \sigma_{21}(\omega - \omega_0) I(\omega, z)} \tag{4.95}$$

where we have used (4.55), and defined the quantities

$$\boxed{n^* = n_2 - \frac{g_2}{g_1} n_1, \quad \sigma_{21}(\omega - \omega_0) = \frac{\pi^2 c^2}{\omega_0^2} A_{21} g_H(\omega - \omega_0)} \tag{4.96}$$

The first of these is known as the *population inversion density*, and is essentially the difference in the populations per state for the two levels. $\sigma_{21}(\omega - \omega_0)$ is known as the *optical gain cross-section*. We also further define the quantity

$$\boxed{\alpha_{21}(\omega - \omega_0) = n^* \sigma_{21}(\omega - \omega_0)} \tag{4.97}$$

This is the *small signal gain coefficient* (units m^{-1}), that is in general a function of beam intensity, as we shall see later. If we assume that the population inversion is positive, stable, and independent of beam position, then we can write the evolution of the beam as

$$I(\omega, z) = I(\omega, 0) e^{\alpha_{21}(\omega - \omega_0) z} \tag{4.98}$$

It is thus clear $\alpha_{21}(\omega - \omega_0)$ is an important parameter that controls the rate of exponential growth of the beam with propagation. The reason for such growth is obvious; the rate of stimulated emission from the upper level is greater than the rate of absorption from the lower level.

A laser operates on a transitions within a diatomic molecule. The upper excited level has a lifetime of 10 *ns against radiative decay that occurs on the laser transition at* 250 *nm to the unstable ground electronic level, which has a lifetime of* 3×10^{-14} *s against dissociation into its constituent atoms. Calculate the following:*

- *The peak optical gain cross-section, assuming pure lifetime broadening*
- *The upper level population density required to produce a small signal gain coefficient of* 0.1 m^{-1}
- *The power per unit volume require to sustain the population calculated above, assuming that* 10% *of input power leads to excitation to the upper level*

We are assuming that the system is entirely lifetime broadened, meaning that we can make use of (4.80) to write the optical gain cross-section as

$$\sigma_{12}(\omega - \omega_0) = \frac{\pi^2 c^2}{\omega_0^2} A_{21} \frac{1}{\pi} \frac{\gamma/2}{(\omega - \omega_0)^2 + (\gamma/2)^2} \tag{4.99}$$

where we note that

$$\gamma = \frac{1}{\tau_1} + \frac{1}{\tau_2} \backsim \frac{1}{\tau_1} \tag{4.100}$$

as the lower level is very short-lived. We are asked to find the *peak* optical gain cross-section; this evidently occurs around the maximum of the Lorentzian at $\omega = \omega_0$. Noting further that $A_{21} \backsim \tau_2^{-1}$, it follows that

$$\sigma_{21}(0) = \frac{\lambda_0^2}{2\pi} \frac{\tau_1}{\tau_2} \backsim 3 \times 10^{-16} \text{ cm}^2 \tag{4.101}$$

The fact that the lower level is very short lived also means that its population will be very low, such that $n_2 \gg n_1 \to n^* \backsim n_2$. Using the definition of the small signal gain coefficient (4.97), it follows that

$$n_2 \backsim \frac{\alpha_{12}(0)}{\sigma_{12}(0)} \backsim 3 \times 10^{-17} \text{ cm}^{-3} \tag{4.102}$$

Using (4.60), and remarking that each excitation to the upper level requires an input of energy $\hbar\omega_0$, it follows that

$$P_2 = R_2 \hbar\omega_0 = \frac{n_2}{\tau_2} \frac{hc}{\lambda_0} \backsim 250 \text{ kW cm}^{-3} \tag{4.103}$$

This is a very large amount of power, too large to be practically sustainable when creating the above laser.

4.4.1 Narrow Band Radiation

For an amplifier (or gain medium) it is often the case that the bandwidth of the beam to be amplified is narrow in comparison to the optical transition concerned. We shall use this simplifying assumption in what follows. The general rate equation for the eupper level can be written in the form

$$\frac{dn_2}{dt} = R_2 - (n_2 B_{21} - n_1 B_{12}) \int_0^\infty d\omega\, \rho(\omega) g_H(\omega - \omega_0) + \dots \tag{4.104}$$

where the total rate of stimulated emission is given by integrating over the lineshape for the transition. $+\dots$ indicates that in general, other terms by appear in the rate equation. This equation can be re-written in the form

$$\frac{dn_2}{dt} = R_2 - n^* \int_0^\infty d\omega\, \sigma_{21}(\omega - \omega_0) \frac{I(\omega)}{\hbar\omega} + \dots \tag{4.105}$$

For narrow band radiation, the gain cross-section varies slowly over the spectral width of the radiation, and so $I(\omega)$ acts as $I(\omega) = I_T\delta(\omega-\omega_L)$, where ω_L is the central frequency of the beam, and I_T is the *total intensity* defined as

$$I_T(z) = \int_0^\infty d\omega\, I(\omega, z) \tag{4.106}$$

It follows that

$$\boxed{\frac{dn_2}{dt} = R_2 - n^*\sigma_{21}(\omega_L-\omega_0)\frac{I_T}{\hbar\omega_L} + \dots} \tag{4.107}$$

We can think of n^* as being the effective number density of the inverted atoms, and $\sigma_{21}(\omega_L-\omega_0)$ as their effective cross-sectional area. Note that $I_T/\hbar\omega_L$ is the incident photon flux.

We have already derived (4.95) that describes the growth of each spectral component of a beam. To describe the rate of growth of a beam of finite spectral width, we integrate both sides over the bandwidth of the beam:

$$\int_0^\infty d\omega\, \frac{\partial I}{\partial z} = \frac{\partial}{\partial z}\int_0^\infty d\omega\, I(\omega,z) = \int_0^\infty d\omega\, n^*\sigma_{21}(\omega-\omega_0)I(\omega,z) \tag{4.108}$$

For narrow band radiation, we once again assume Delta-function behaviour. Using (4.106), we find that

$$\boxed{\frac{dI_T}{dz} = n^*\sigma_{21}(\omega_L-\omega_0)I_T} \tag{4.109}$$

4.4.2 Gain Saturation

From now on, we shall adopt the notation $I = I_T$ unless stated otherwise. Let us now look at the level populations of a laser operating under steady-state conditions in the presence of an intense, narrow-band radiation. By analogy to (4.107), we can write the rate equations as

$$\frac{dn_2}{dt} = R_2 - n^*\sigma_{21}(\omega_L-\omega_0)\frac{I}{\hbar\omega_L} - \frac{n_2}{\tau_2} \tag{4.110}$$

$$\frac{dn_1}{dt} = R_1 + n^*\sigma_{21}(\omega_L-\omega_0)\frac{I}{\hbar\omega_L} + n_2A_{21} - \frac{n_1}{\tau_1} \tag{4.111}$$

We assume that R_1 and R_2 are constant, independent of n_1 and n_2, and include both direct (collision excitation) and indirect (radiative pumping, or non-radiative cascades) processes. Taking the steady state solutions of these equations, and eliminating n_1 and n_2, we obtain

$$n^* = \frac{R_2\tau_2[1-(g_2/g_1)A_{21}\tau_1] - (g_2/g_1)R_1\tau_1}{1+\sigma_{21}\frac{I_T}{\hbar\omega_L}[\tau_2 + (g_2/g_1)\tau_1 - (g_2/g_1)A_{21}\tau_1\tau_2]} \tag{4.112}$$

Inspecting the above expression, it is clear that the denominator is equal to unity for $I = 0$, meaning that the numerator must be the population inversion produced by the pumping in the absence of the beam. We can thus re-write the above equation as

$$\boxed{n^*(I) = \frac{n^*(0)}{1+I/I_S}} \tag{4.113}$$

We introduce the parameters

$$\boxed{I_S = \frac{\hbar\omega_L}{\sigma_{21}\tau_R}, \quad \tau_R = \tau_2 + \frac{g_2}{g_1}\tau_1[1-A_{21}\tau_2]} \tag{4.114}$$

which are known as the *saturation intensity* and *recovery time* respectively. The application of the intense, narrow-band radiation thus reduces the population inversion by a factor of $(1 + I/I_S)$. as a result of the increased rate of stimulated emission from the upper laser level. The saturation intensity is a measure of the intensity required to reduce the population inversion to one half of that which is achieved in the absence of the beam. The saturation intensity also depends on the detuning of the intense radiation from the centre frequency of the transition through the optical cross-section. This is because the interaction is stronger for $\omega_L \backsim \omega_0$, and so a lower (saturation) intensity is required to transfer population from the lower to the upper level.

We also define the *saturated gain coefficient* as

$$\boxed{\alpha_I(\omega - \omega_0) = \frac{\alpha_{21}(\omega - \omega_0)}{1 + I/I_s}} \tag{4.115}$$

where $\alpha_{21}(\omega - \omega_0)$ is the small signal gain coefficient. We can examine a few simple cases of this expression, imagining that we measure $\alpha_I(\omega - \omega_0)$ under different conditions:

(i) Using a weak, tunable probe beam with $I = 0$ - In this case, we would expect the saturation gain coefficient to be equal to the small signal gain coefficient, as given by (4.115). Thus means that α_I is simply related to a Lorentzian lineshape $g_H(\omega - \omega_0)$ by (4.96) and (4.97)

(ii) Using a weak probe beam with a narrow band beam of intensity $I = I_s$. By the definition of the saturation intensity, the population will be reduced by a factor of a half, such that $\alpha_I = \alpha_{21}/2$.

(iii) Using an intense, narrow band beam of constant intensity $I = I_s(0)$. The intensity of the beam is tuned to $\omega_L = \omega_0$, meaning that at this point, $\alpha_I = \alpha_{21}/2$. However, at larger values of ω (that is, larger detuning), the probe beam intensity is small in comparison to the saturation intensity, and hence only disturbs their populations slightly. This gives rise to the curve shown below. Using the definitions of α_{21} and I_s, it can be shown that this is another Lorentzian of FWHM

$$\Delta\omega_I = \Delta\omega_H \sqrt{1 + \frac{I}{I_s(0)}} \tag{4.116}$$

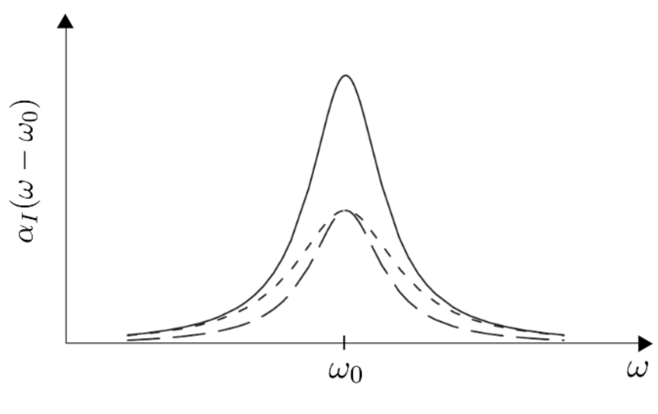

Figure 4.5: A graph of $\alpha_I(\omega - \omega_0)$ for the cases (i) (solid line), (ii) (larger dashed line) and (iii) (smaller dashed line)

4.4.3 Beam Growth

Our intensity equation (4.109) states that

$$\frac{dI}{dz} = \alpha_I I = \frac{\alpha_{21}}{1 + I/I_s} I \tag{4.117}$$

which can be integrated to give

$$\boxed{\log\left[\frac{I(z)}{I_0}\right] + \frac{I(z) - I_0}{I_s} = \alpha_{21} z} \tag{4.118}$$

This equation is transcendental, and does not have a general analytical solution. However, we have the two limits that

$$I(z) = I_0 e^{\alpha_{21} z} \quad \text{for } I(z) \ll I_s \text{ (weak beam)} \tag{4.119}$$

$$I(z) = I_0 + \alpha_{21} I_s z \quad \text{for } I_0 \gg I_s \text{ (heavy saturation)} \tag{4.120}$$

That is, at low intensities, the beam grows exponentially with distance, but once the laser transition becomes heavily saturated, the intensity grows linearly. Note that we can approximate $\tau_R \backsim \tau_2$ for predominantly radiative transitions ($A_{21} \backsim \tau_2^{-1}$), and that $n^* \backsim n_2 \backsim R_2 \tau_2$ for a short groundstate lifetime with upper level pumping rate R_2. This allows us to obtain approximate expressions for I_s and α_{21}.

4.5 Cavity Effects and Lasers

A simple laser amplifier consists of one or more sections of inverted media such that a beam injected into it will be amplified as it propagates. In a laser oscillator, the grain medium is located within an optical cavity, such that the laser radiation originates within the gain medium, and is amplified as it circulates around the optical cavity. Such optical cavities behave in a very similar way to the Fabry-Perot interferometer; we can calculate the *longitudinal cavity modes* from the maxima of the Airy function, or remark that the modes must satisfy

$$2kn\ell = 2\pi p \quad \longrightarrow \nu_p = \frac{c}{2n\ell}p \tag{4.121}$$

where n is the refractive index of the medium, and L is the cavity length. Now, let us assume that the gain is uniform throughout the cavity. In the absence of losses, beam will then experience a growth

$$e^{2\ell\kappa(\omega-\omega_0)} \tag{4.122}$$

where $\kappa(\omega-\omega_0)$ is the *absorption coefficient*. Losses will come from exponential absorption proportional to $\alpha_{21}(\omega-\omega_0)$, and imperfect reflection off the inside surfaces of the cavity, taken into account using the power reflectivities R_1 and R_2. Putting these together, we write that

$$R_1R_2e^{2\ell[\kappa(\omega-\omega_0)-\alpha_{21}(\omega-\omega_0)]} = 1 \tag{4.123}$$

The threshold condition for laser operation occurs where the round-trip gain $\kappa(\omega-\omega_0)$ is zero, resulting in the expression

$$\boxed{\alpha_{21}(\omega-\omega_0) = \frac{1}{2\ell}\log\left[\frac{1}{R_1R_2}\right]} \tag{4.124}$$

This is essentially a statement that for laser oscillations to occur for some cavity mode corresponding to the frequency ω, the unsaturated round-trip gain inside the cavity exceeds the round-trip loss.

4.5.1 Lasers

In the material above, we have studied the laser as a two level atomic system. However, it turns out that two level systems cannot display laser behaviour as they cannot achieve a population inversion. Consider a system for which $g_1 = g_2$ and the total number density is given by $n = n_1 + n_2$, and $n^* = 2n_2 - n$. From (4.110) in the steady state, and assuming that $A_{21} \backsim \tau_2^{-1}$, it is easy to show that

$$n_2 = \frac{R_2}{2\frac{\sigma_{21}I}{\hbar\omega_L} + A_{21}} + \frac{n}{2 + \frac{A_{21}\hbar\omega_L}{\sigma_{21}I}} \tag{4.125}$$

From this expression, it is clear that the maximum population that we can achieve on the upper level is $n_2 = n/2$; increasing the input intensity, optical gain cross-section, or pumping rate cannot achieve this (as the former two increase with the latter). This means that more levels are required in order to exhibit laser behaviour. For simplicity, we shall continue to assume that $g_1 = g_2$.

Three Level Lasers

The three level laser is the system behind the famous ruby laser. In a three level laser, population is pumped to the third level from the lowest level at a rate $\Gamma_{13}n_1$, which then rapidly decays *non-radiatively* to the second level, from which the laser transition occurs.

The rapid decay is usually through collisional decay, so we denote the timescale for this process τ_c. Define the radiative decay coefficients for the upper and middle levels as $A_{31} \backsim \tau_3^{-1}$ and $A_{21} \backsim \tau_2^{-1}$ respectively.

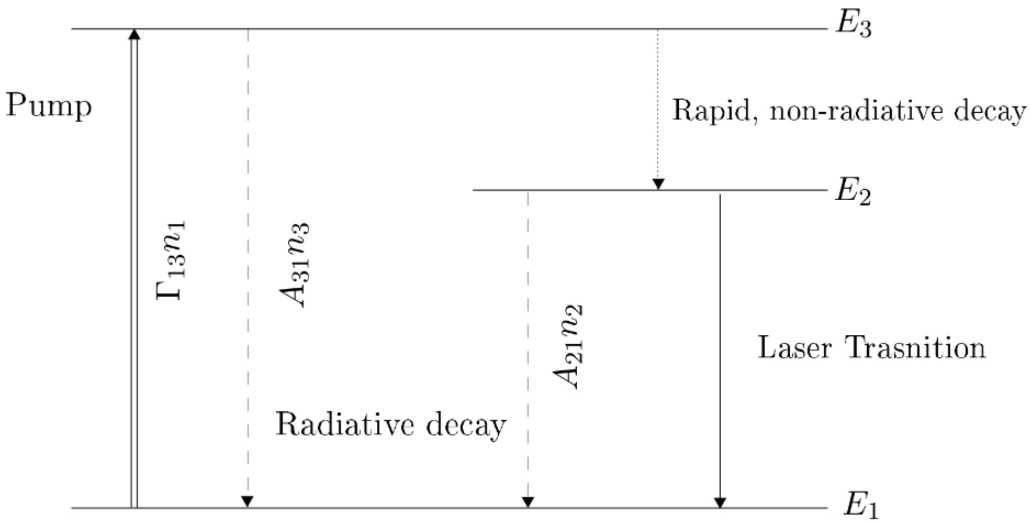

Figure 4.6: A schematic diagram for a three level laser system

We can then write the rate equations

$$\frac{dn_3}{dt} = \Gamma_{31}n_1 - A_{31}n_3 - \frac{n_3}{\tau_c} \tag{4.126}$$

$$\frac{dn_2}{dt} = -n^*\sigma_{21}\frac{I}{\hbar\omega_L} - A_{21}n_2 + \frac{n_3}{\tau_c} \tag{4.127}$$

$$\frac{dn_3}{dt} = -\Gamma_{31}n_1 + n^*\sigma_{21}\frac{I}{\hbar\omega_L} + A_{21}n_2 + A_{31}n_3 \tag{4.128}$$

Using the population relations $n = n_1 + n_2 + n_3$ and $n^* = n_2 - n_1$, we find that

$$\frac{n_2}{n_1} = \frac{\frac{\Gamma_{13}}{\tau_c} + \left(A_{31} + \frac{1}{\tau_c}\right)\sigma_{21}\frac{I}{\hbar\omega_L}}{\left(A_{31} + \frac{1}{\tau_c}\right)\left(\sigma_{21}\frac{I}{\hbar\omega_L} + A_{21}\right)} = \frac{\frac{\Gamma_{13}}{\tau_c} + \left(A_{31} + \frac{1}{\tau_c}\right)\frac{I}{\tau_R I_s}}{\left(A_{31} + \frac{1}{\tau_c}\right)\left(\frac{I}{\tau_R I_s} + A_{21}\right)} \tag{4.129}$$

Let us work in the regime where the intensity is much smaller than saturation intensity, meaning that we can disregard terms including a factor I/I_s:

$$\boxed{\frac{n_2}{n_1} = \frac{\frac{\Gamma_{13}}{\tau_c}}{\left(A_{31} + \frac{1}{\tau_c}\right)A_{21}} \backsim \frac{\Gamma_{13}}{A_{21}} > 1} \tag{4.130}$$

The last expression follows from the assumption that the decay from the upper to the middle level is very quick, such that $n_3 \backsim 0$, and $A_{31}\tau_c \ll 1$. As we would expect, the condition for population inversion is that the pump rate is higher than the laser decay rate; we can treat the upper level as almost not even being there.

Let us derive an expression for the threshold energy that has to be supplied to the pump in order to sustain a population inversion. In the limit of $\tau_c \ll \tau_3, \tau_2$, we can approximate that at the threshold:

$$n = n_1 + n_2 \tag{4.131}$$

$$n_{th}^* = n_2^{th} - n_1^{th} \tag{4.132}$$

Then

$$n_2^{th} = \frac{n + n_{th}^*}{2} \backsim \frac{n}{2} \tag{4.133}$$

The energy is given by

$$\begin{aligned} E^{th} &= \{\text{upper population density}\} \times \{\text{volume}\} \times \{\text{energy per particle}\} && (4.134) \\ &= n_2^{th}(\pi a^2 \ell)\frac{hc}{\lambda_p} && (4.135) \end{aligned}$$

where λ_p is a the wavelength corresponding to a particular cavity mode ν_p as given by (4.121), and a is the radius of the laser cavity. Given (4.133), we can write the final expression of

$$\boxed{E_{(3)}^{th} = \frac{n}{2}(\pi a^2 \ell)\frac{hc}{\lambda_p}} \tag{4.136}$$

Four Level Lasers

Four level lasers are more efficient than three level lasers. This is achieved through the addition of a fourth additional level *below* the lowest laser level that allows level 1 to quickly empty via collisional decay into level 0, making it easier to obtain a population inversion between levels 1 and 2 (the laser levels). In this case, we assume rapid collisional decay between the pairs of levels 3 and 2, and 0 and 1, such that $A_{21} \ll \tau_1^{-1}, \tau_3^{-1}$. Let τ_0 be the rate of absorption for the lowest level.

Under the condition that the laser intensity is small, we can ignore the laser transition terms as they contain factors of I/I_s. This means that the rate equations for the four levels can then be written as:

$$\begin{aligned} \frac{dn_3}{dt} &= \Gamma_{03}n_0 - \frac{n_3}{\tau_3} && (4.137) \\ \frac{dn_2}{dt} &= -A_{21}n_2 + \frac{n_3}{\tau_3} && (4.138) \\ \frac{dn_1}{dt} &= A_{21}n_2 - \frac{n_1}{\tau_1} + \frac{n_0}{\tau_0} && (4.139) \\ \frac{dn_0}{dt} &= -\Gamma_{03}n_0 - \frac{n_0}{\tau_0} && (4.140) \end{aligned}$$

Noting that now $n = n_0 + n_1 + n_2 + n_3$ and $n^* = n_2 - n_1$, the steady state populations can be written as

$$n_2 = \frac{\Gamma_{03}}{A_{21}}n_0, \quad n_1 = \frac{\Gamma_{03} + \frac{1}{\tau_0}}{\frac{1}{\tau_1}}n_0, \quad \frac{n_2}{n_1} = \frac{\frac{\Gamma_{03}}{\tau_1}}{A_{21}\left(\Gamma_{03} + \frac{1}{\tau_0}\right)} \tag{4.141}$$

Since the levels 0 and 1 are in collisional equilibrium, we must have that $n_0/\tau_0 = n_1/\tau_1$, which implies that

$$\frac{n_1}{n_0} = \frac{\tau_1}{\tau_0} \backsim e^{-\beta\hbar\omega_{10}} \tag{4.142}$$

We also typically have that $A_{21} \ll \tau_1^{-1}$, as above. The condition for population inversion is if the last expression in (4.141) is greater than one, which we can re-write as

$$\boxed{\Gamma_{03} > A_{21}e^{-\beta\hbar\omega_{10}}} \tag{4.143}$$

We can see that in the case of the four level laser system, the pumping requirements are reduced by this exponential factor that depends on the energy difference $\hbar\omega_{10}$ between the levels 0 and 1. Note that we have not made any assumptions about the magnitude of this energy difference.

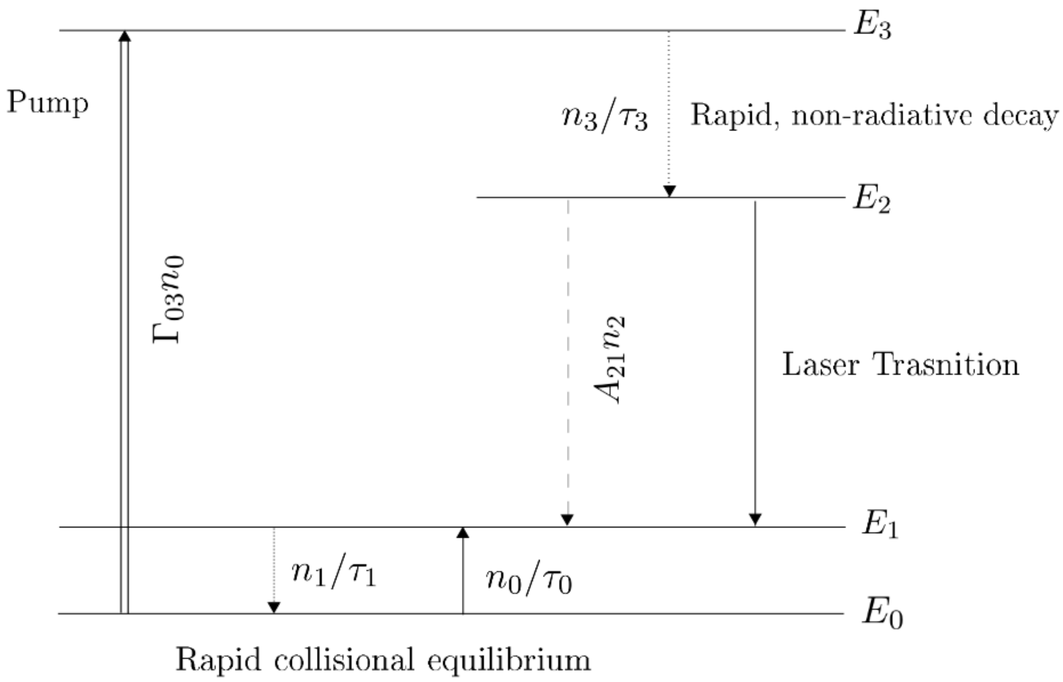

Figure 4.7: A schematic diagram for a four level laser system

A four level laser system such as this forms the basis for the Nd:YAG laser. If the energy gap $\hbar\omega_{10}$ is sufficiently large, we can approximate that $n_1 \backsim n_3 \backsim 0$. This means that the population inversion at threshold is approximately equal to the population of the upper laser level $n_2^{th} \backsim n_{th}^*$. By the same logic as before, the threshold energy for a four level laser is given by

$$\boxed{E_{(4)}^{th} = n_{th}^*(\pi a^2 \ell)\frac{hc}{\lambda_p}} \tag{4.144}$$

Given appropriate information, it is possible to calculate an expression for n_{th}^* using (4.124). If one compares the magnitudes of (4.136) and (4.144), it becomes obvious that $E_{(4)}^{th} \ll E_{(3)}^{th}$; that is, they are much more efficient.

In practise, however, these values are much smaller than the actual electric energy that has to be applied to maintain laser operation. It is in fact larger by $\backsim \times 60$, due to the following factors:

- $\times 2$ - To achieve pumping within the laser rod, the doping and diameter must be such that only 50% of the pump photons are actually absorbed
- $\times 8$ - Only about 12% of the output of the flashlamp will lie in the range of the pump band
- $\times 2$ - Only about 50% of the pump light is geometrically coupled into the rod
- $\times 1.7$ - Only about 60% of the electrical energy supplied is actually converted into light

This means that quite a lot more electrical energy must be supplied than the threshold energy in practise.